COMMONWEALTH OF PENNSYLVANIA
DEPARTMENT OF TRANSPORTATION

PENNDOT RESEARCH

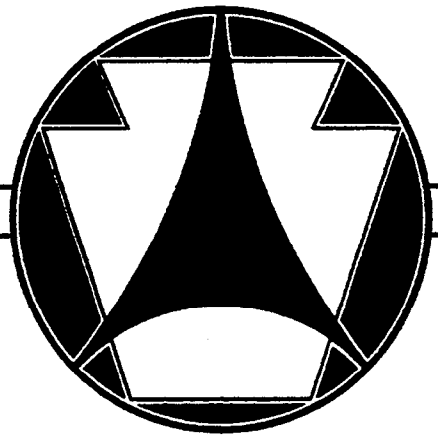

EVALUATION OF TRIAXIAL STRENGTH AS A SIMPLE TEST FOR ASPHALT CONCRETE RUT RESISTANCE

University-Based Research, Education and Technology Transfer Program
AGREEMENT NO. 359704, WORK ORDER 19

FINAL REPORT

AUGUST 2000

By D. W. Christensen, R. Bonaquist, and D. P. Jack

PENNSTATE

1855

Pennsylvania Transportation Institute

The Pennsylvania State University
Transportation Research Building
University Park, PA 16802-4710
(814) 865-1891 www.pti.psu.edu

REPORT DOCUMENTATION PAGE

Form Approved OMB NO. 0704-0188

1. Agency Use Only (Leave Blank)	2. Report Date	3. Report Type and Dates Covered
	August 31, 2000	Final Report 4/12/99 – 8/31/00

4. Title and Subtitle
Evaluation of Triaxial Strength as a Simple Test for Asphalt Concrete Rut Resistance

5. Funding Numbers
Agreement No. 359704
Work Order No. 19

6. Author(s)
Donald W. Christensen, Ramon Bonaquist, Donald P. Jack

7. Performing Organization Name(s) and Address(es)
The Pennsylvania State University
The Pennsylvania Transportation Institute
201 Transportation Research Building
University Park, PA 16802-4710

8. Performing Organization Report No.
2K26

9. Sponsoring/Monitoring Agency Name(s) and Address(es)
Pennsylvania Department of Transportation
Bureau of Planning and Research
Division of Research
555 Walnut Street-6th Floor Forum Place
Harrisburg, PA 17101-1900

10. Sponsoring/Monitoring Agency Report Number
FHWA-PA-2000-010+97-04 (19)

11. Supplementary Notes
COTR: Dean Maurer, 717-787-5229

12a. Distribution / Availability Statement
Available from National Technical Information Service, Springfield, VA

12b. Distribution Code
N/A

13. Abstract (Maximum 200 words)

The purpose of this study was to evaluate the use of triaxial strength testing as a simple performance test for evaluating the rut resistance of asphalt concrete mixtures. A total of ten dense-graded asphalt concrete mixtures were tested using standard triaxial strength tests, which involved performing unconfined and confined strength tests on specimens cored from gyratory samples. An abbreviated protocol was also used to characterize the mixtures, which involved direct testing of gyratory specimens in compression and indirect tension (IDT). Six of the mixtures were based on Marshall mix designs placed in Pennsylvania, and four were based upon Superpave mix designs placed in New York State. A significant range in binder grades, aggregate types, and aggregate gradations were represented. It was found that the abbreviated protocol provided more precise estimates of the Mohr-Coulomb failure parameters than the standard triaxial procedure, especially for the cohesion parameter, which can be estimated accurately from the IDT strength. The mixture cohesion was found to relate very well to mixture rut resistance. The IDT strength was found to be an excellent predictor of rut resistance, and is very promising as a simple and effective test for quality control, acceptance testing, and mixture design and analysis.

14. Subject Terms
asphalt concrete, rut resistance, triaxial strength, Mohr-Coulomb failure parameters, internal friction, cohesion, Superpave shear test, performance testing

15. No. of Pages

16. Price Code
N/A

17. Security Classification of Report	18. Security Classification of this Page	19. Security Classification of Abstract	20 Limitation of Abstract
None	None	None	None

EVALUATION OF TRIAXIAL STRENGTH AS A SIMPLE TEST FOR ASPHALT CONCRETE RUT RESISTANCE

University-Based Research, Education and Technology Transfer Program
Agreement No. 359704
Work Order 19

FINAL REPORT

Prepared for

Commonwealth of Pennsylvania
Department of Transportation

By

Donald W. Christensen, Ramon Bonaquist, and Donald P. Jack

The Pennsylvania Transportation Institute
The Pennsylvania State University
Transportation Research Building
University Park, PA 16802-4710

August 31, 2000

This work was sponsored by the Pennsylvania Department of Transportation and the U.S. Department of Transportation, Federal Highway Administration.

PTI 2K26

ACKNOWLEDGEMENTS

The authors would like to thank the following people and their organizations for their help in gathering the materials and data used in completing this research:

- Gayle King and Ron Kohler, Koch Materials Company;
- Frank Fee, Citgo Asphalt Company;
- Tim Ramirez and Dean Maurer, The Pennsylvania Department of Transportation;
- Roger Studer, Hempt Brothers;
- Ron Sines, Zoab Ziveri and Chris Euler, New York Department of Transportation; and
- Greg Harders, Cortland Asphalt Company.

The work presented within this report does not necessarily reflect the points of view of any of these individuals or their organizations, including the Pennsylvania Department of Transportation.

TABLE OF CONTENTS

LIST OF TABLES

LIST OF FIGURES

1. INTRODUCTION

The purpose of this report is to document research meant to evaluate the usefulness of triaxial strength testing as a simple performance test for evaluating the rut resistance of asphalt concrete mixtures. Although the Superpave mixture and analysis system has been very successful in developing durable mix designs, many engineers and technicians feel that a simple performance, or "proof," test is needed to ensure adequate performance for asphalt concrete mixtures. Of special concern is resistance to permanent deformation. Triaxial strength testing is attractive as a simple performance test for rut resistance. It is relatively quick, simple, and inexpensive, and its simplicity should ensure good repeatability. Furthermore, triaxial strength testing provides information concerning mixture cohesion and internal friction, both of which should contribute to mixture rut resistance. To provide an even simpler test, the research team evaluated as part of this project an abbreviated protocol for triaxial testing, which involved direct testing of gyratory specimens using IDT strength and unconfined compression procedures. This approach is especially attractive for routine use by engineers and technicians working in the field designing and analyzing mixtures and performing QC/QA tests.

Currently, a large research effort is underway as part of NCHRP Project 9-19 to evaluate a number of simple performance candidate tests, including triaxial strength (University of Maryland, 1998). The research summarized in this report, although similar to that done as part of NCHRP 9-19, differs in several significant respects. The testing conditions—temperature and loading rate—were carefully selected in this study to provide rheologically equivalent conditions to those existing under a pavement subjected to traffic loading. These conditions are substantially different from those selected by the NCHRP 9-19 research team. Another important difference is, of course, the evaluation of the abbreviated protocol, which is not under consideration by NCHRP 9-19. The work performed during this project and documented in this report should therefore not be considered redundant to that done as part of NCHRP Project 9-19.

This project involved testing 10 different mixtures. Six of these were used on a research project performed by the Pennsylvania Department of Transportation, in which various mixtures were placed on State Route 11 (S.R. 11) south of Harrisburg, Pennsylvania, to evaluate their relative resistance to rutting under very heavy traffic (Fee, 1993; Ramirez, 1995). These mixtures were designed using the Marshall mix-design procedure and involved two different

gradations and two different binders, one polymer modified and one conventional. The other four mixtures were part of a New York Department of Transportation Superpave implementation study and were included in a research study on N_{design} performed by the Asphalt Institute (Anderson et al., 1999). These mixtures were placed on four different highways in New York State; well-documented rut measurements were available for the S.R. 11 mixtures but not for the New York N_{design} mixtures. To provide for further evaluation of the triaxial strength data, repeated shear at constant height (RSCH) tests were also performed on all mixtures. Care should be taken in interpreting these results and extending them to strength tests performed using methods other than those used in this project. The results of both compressive strength tests and IDT tests are dependent on test temperature and loading rate. Careful consideration should be given to test conditions when comparing strength data from different sources or when comparing strength data with field performance or dynamic test data.

2. BACKGROUND

2.1. Permanent Deformation, The Superpave System, and Simple Performance Tests

Rutting, or permanent deformation, is one of the main failure mechanisms for asphalt concrete pavements. Excessive permanent deformation can occur in mixtures that lack adequate stiffness and/or strength at high temperatures. Significant rutting normally only occurs during hot weather, when the surface of flexible pavements can reach a temperature of 60 °C or higher. Furthermore, this mode of distress is also associated with relatively high traffic levels—the greater the number of vehicles, and the greater the proportion of heavy trucks, the greater the potential for permanent deformation. Rutting is a serious problem for a number of reasons; rain or melted snow and ice can pond in the ruts, increasing the chance for vehicle hydroplaning and subsequent accidents. Permanent deformation is also often associated with flushing or bleeding, where asphalt binder rises to the surface of the pavement, creating a very smooth surface. This can reduce tire-pavement friction, especially when wet, again increasing the potential for accidents. Excessive ruts can also reduce the effective thickness of a pavement, reducing the structural capacity of the pavement and increasing the likelihood of premature failure through fatigue cracking.

Several approaches have been used to design rut-resistant hot-mix asphalt concrete (HMAC) mixtures. Almost all asphalt concrete design methods have included some means of grading and selecting the asphalt binder to help produce rut-resistant mixtures. Currently, the PG-grading method used in the Superpave system uses the design high pavement temperature, which can be thought of as a high service temperature for a given binder. A PG 64-22 binder, for example, can be used in mixtures subjected to 7-day average high pavement temperatures of up to 64 °C under normal traffic conditions (The Asphalt Institute, 1996). A second important aspect of designing rut resistant mixtures is the selection of aggregates of good quality and proper gradation. In the Superpave system, four aggregate consensus properties ensure adequate quality: coarse aggregate angularity, fine aggregate angularity, flat/elongated particles, and clay content (The Asphalt Institute, 1996). The Pennsylvania Department of Transportation has numerous additional aggregate quality requirements (PennDOT, 1994). The Superpave system of mix design also has specific aggregate gradation requirements, largely developed on the basis of experience to provide mixtures with good rut resistance. One important aspect of Superpave

gradations is the restricted zone, which discourages the use of aggregate blends with gradations approaching maximum density in the sand-sized particle range (The Asphalt Institute, 1996). In general, experience during the past twenty years suggests that significant deviation from maximum density gradations helps to produce rut-resistant asphalt concrete mixtures.

Perhaps the most important aspect of designing rut-resistant HMAC mixtures is the selection of the optimum binder content. In the Superpave mix design system, asphalt concrete specimens having a range of binder contents are prepared using a gyratory compactor. The design binder content is that producing 4 % air voids at the appropriate level of compaction. The level of compaction, determined by the design number of gyrations (N_{design}), is directly related to the design traffic level as quantified by equivalent single axle loads, or ESALs (The Asphalt Institute, 1996).

The Superpave system, unlike its predecessor the Marshall mix design method, originally included no strength or stiffness test as a final step in evaluating paving mixtures. Many practicing pavement engineers and technicians were uncomfortable with this lack of a "proof" test. Furthermore, unexpected premature rutting in some mixtures at the WesTrack project indicated that the Superpave system was perhaps not completely reliable in producing rut-resistant asphalt concrete mixtures. Therefore, much attention has been given over the past several years to developing a simple performance test, primarily for the purpose of evaluating the rut-resistance of asphalt concrete mixtures designed using the Superpave system. One of the main tasks of NCHRP Project 9-19, being executed at Arizona State University, is to evaluate a number of candidate simple performance tests and select the most promising (University of Maryland, 1998). The triaxial strength test is one of the tests being evaluated by NCHRP 9-19; in fact, the research team for this project originally was to perform this evaluation, but the NCHRP 9-19 research team later decided to do this evaluation internally. The research reported here has continued, since this project addresses several technical issues outside the scope of NCHRP Project 9-19.

The research team believes that the work presented in this report is unique and involved little duplication of the NCHRP 9-19 effort. A significantly greater amount of time and resources could be devoted to a careful evaluation of the triaxial strength test in this project. The testing conditions used were carefully selected to provide approximately rheologically equivalent conditions to traffic loading at high temperatures and were considerably different from those

used in NCHRP 9-19. Furthermore, more attention was given to analysis of the resulting data, and potential application of the triaxial strength test as a mix design tool, and not just a simple proof test. Another unique feature of this work was the evaluation of a simplified protocol for determining triaxial strength failure parameters involving only compression and split tension testing of unmodified gyratory specimens. In summary, the research presented in this report is significantly different from, and in some ways more detailed than, the corresponding research performed by NCHRP Project 9-19.

2.2. Triaxial Strength Testing and Mohr-Coulomb Failure Parameters

Triaxial strength testing is essentially a method for evaluating the effects of confining pressure on the strength of granular materials. This technique was original developed by soils engineers and scientists and is closely associated with the Mohr-Coulomb failure theory.

A clean, purely granular material such as sand, without any confining pressure, has no strength—it cannot even support its own weight, other than in a pile within which internal stresses provide effective confinement. Sandy soils can support stresses because the weight of the sand, and the applied stress of a footing or any other load, produces confining stresses which results in significant strength. Soils that are partly cohesive and partly granular will exhibit some strength without confinement but will exhibit even greater strength under confining stresses; thus, in soils engineering, it is essential to understand the effect of confining stresses on the strength of any given soil. The triaxial strength test was developed to determine the effect of confining pressure on the strength of soils.

In a typical triaxial strength test, a soil specimen is prepared for testing with an aspect ratio of 2 to 1 (height to diameter); the actual specimen dimensions vary from approximately 50 mm by 100 mm to 100 mm by 200 mm. The specimen is encased in a latex membrane and placed inside a specially designed pressure vessel, called a triaxial cell, in which pressure can be applied to the specimen while applying a compressive load. Triaxial cells for soil testing also have provisions for keeping a specimen saturated and controlling the internal pore water pressure during the test (called "back pressure"), although this is usually not an essential part of triaxial strength testing for paving materials. Figure 1 is a diagram of a typical triaxial cell as used in testing soils.

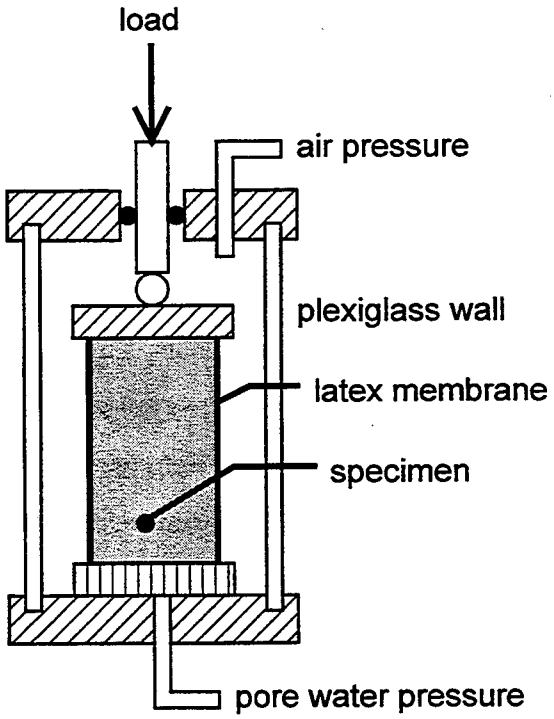

Figure 1. Diagram of Typical Triaxial Cell as Used in Soil Testing.

In analyzing triaxial strength tests, Mohr-Coulomb failure theory is usually applied. This theory is simply a way of mathematically representing the relationship between a confining stress and failure stress for granular materials. Mathematically, it is represented using the following equation (Bowles, 1979):

$$\sigma_1 = \sigma_3 \tan^2\left(45° + \frac{\phi}{2}\right) + 2c \tan\left(45° + \frac{\phi}{2}\right), \quad (1)$$

where:

σ_1 = major principle stress at failure (failure stress plus confining pressure), Pa;

σ_3 = minor principle stress (confining pressure), Pa;

ϕ = angle of internal friction ("phi"), degrees; and

c = cohesion, Pa.

The internal friction is an important parameter for granular materials, indicating the degree of interaction among particles. Granular materials consisting of strong, cubicle aggregates will have a high value for ϕ, indicating a strong dependence of strength on confining stress.

Materials consisting of smooth, spherical particles will have small values for ϕ, indicating little or no increase in strength with confining stress. Obviously, for most engineering applications, a high value of internal friction is more desirable. The cohesion, c, theoretically represents the shear strength at zero confining pressure. For purely granular materials, $c = 0$; for materials containing clay or other plastic fines, the cohesion will have some positive value. Under confinement, the strengths of materials containing both plastic fines and granular materials will depend upon both the cohesion and the internal friction, as suggested by Equation 1 (Bowles, 1979).

The Mohr-Coulomb failure theory is often represented graphically by plotting a series of Mohr's circles representing stress states at incipient failure under increasing levels of confining stress and then drawing a tangent to these circles, which represents the Mohr-Coulomb failure envelope. Figure 2 is a sketch graphically explaining the Mohr-Coulomb failure theory (Bowles, 1979).

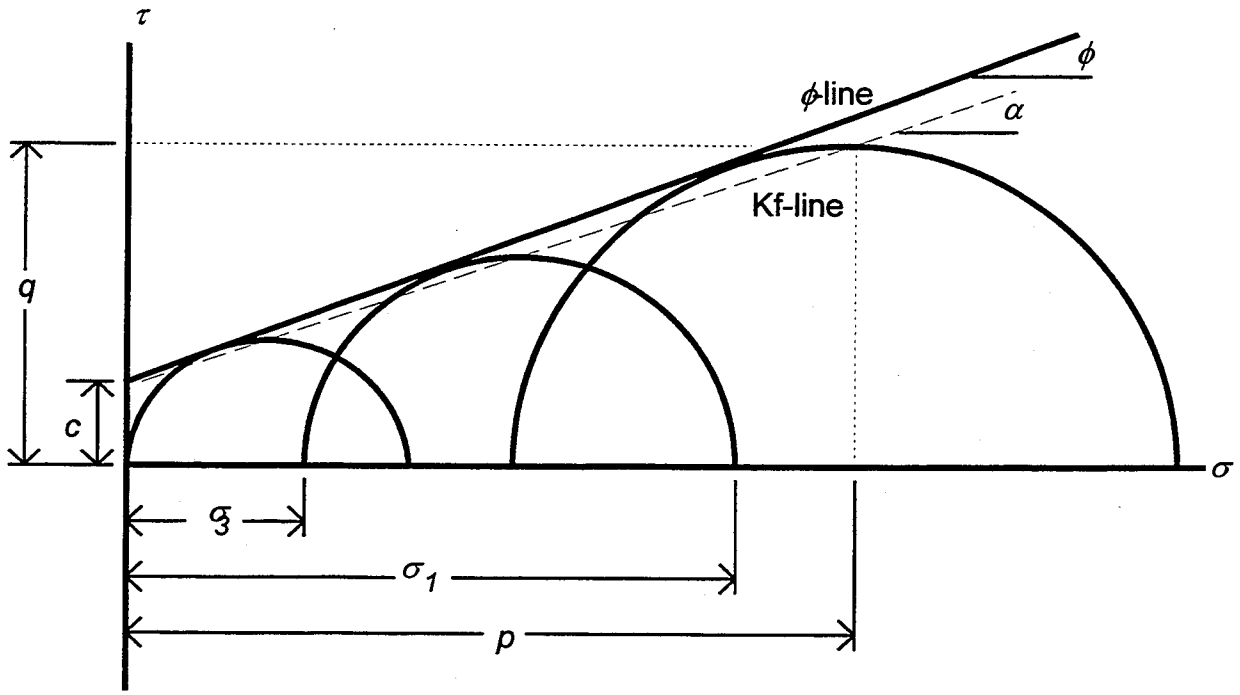

Figure 2. Mohr-Coulomb Failure Theory.

Note that in Figure 2, there are two lines associated with the failure envelope. The first, as described above, is the ϕ-line, tangent to each of the three Mohr's circles shown in the sketch. The second line, called the K_f-line, passes through the maximum shear stress for each Mohr's circle. The coordinates of the maximum shear stress are referred to as p and q, representing the average of the normal stresses and the maximum shear stress, respectively. Mathematically, p and q are given by the following equations (Bowles, 1979):

$$p = \frac{\sigma_1 + \sigma_3}{2} \tag{2}$$

$$q = \frac{\sigma_1 - \sigma_3}{2}, \tag{3}$$

where the variables are as defined previously. In practice, when analyzing triaxial strength data, failure points for each of several tests are converted to p, q coordinates using Equations 2 and 3. Next, linear regression analysis is used to determine the intercept, a_0, and slope, a_1, of the resulting K_f-line. Then, the values for internal friction and cohesion are calculated from these parameters:

$$\phi = \sin^{-1}(a_1) \tag{4}$$

$$c = \frac{a_0}{\cos\phi}, \tag{5}$$

where the variables are as defined previously.

Ultimately, the practical significance of the triaxial failure parameters c and ϕ is that these are used in soils engineering to calculate the bearing capacity of footings. Two well-known and similar methods for calculating bearing capacity of shallow foundations are Terzaghi's equations and Hansen's equation (1). As an example, Equation 6 represents Terzaghi's equation for the ultimate bearing capacity of square footings (Bowles, 1979):

$$q_{ult} = 1.3cN_c + \gamma DN_q + 0.4\gamma BN_\gamma, \tag{6}$$

where:

q_{ult} = ultimate bearing capacity, Pa;

c = soil cohesion, Pa;

D = footing depth, m;

B = footing width, m; and

N_i = bearing capacity factors.

Although this discussion was limited to soils, as will be discussed below, much of this theory is directly applicable to asphalt concrete pavement at intermediate-to-high temperatures. Under these conditions, the mechanical behavior of asphalt concrete is in many ways similar to a cohesive, granular soil. The discussion in the following section will review in some detail the manner in which triaxial strength testing and Mohr-Coulomb failure parameters can be applied to mixture design and analysis.

Mohr-Coulomb failure parameters can also theoretically be determined by performing one set of tests in unconfined compression and a second set in either simple tension or split tension. The latter approach is more practical since soils and granular composites like concrete are difficult to test in pure tension. The Mohr-Coulomb failure parameters for rocks are sometimes determined in this way, by testing in unconfined compression and split tension. Figure 3 represents the construction of Mohr's circles and the associated Mohr-Coulomb failure envelope using this approach. In this diagram, the Mohr's circle farthest to the left represents the state of stress for the split tension tests; σ_x represents the tensile (horizontal) stress at failure, while σ_y represents the compressive (vertical) stress at failure. For a Poisson's ratio of 0.5, $\sigma_y = 3\sigma_x$. The larger Mohr's circle represents the state of stress during the unconfined compression test. The construction of the failure envelope and the calculation of the Mohr-Coulomb failure parameters proceeds in the same way as for data gathered using compression data only.

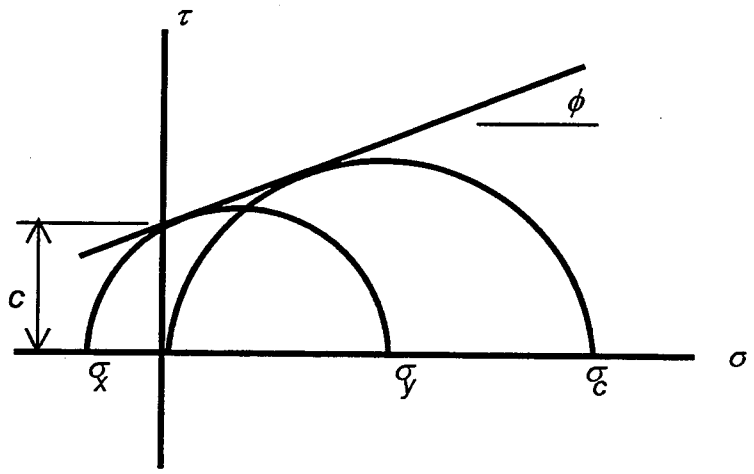

Figure 3. Determination of Mohr-Coulomb Failure Parameters Using Unconfined Compression and Split Tension Data.

The advantage of using compression/split tension data to determine Mohr-Coulomb failure parameters is primarily one of convenience. Using this technique, a triaxial cell is not needed since none of the tests require sconfining pressure. Furthermore, for asphalt concrete, the split tension test is quite widely used and can be performed using a specimen directly out of the gyratory compactor without further modification. The research team believes that the compression test can also be performed directly on a gyratory specimen with reasonable results, if a 150-by-150-mm specimen is used and if the end conditions are carefully controlled to reduce the effective degree of confinement at the ends. Thus, using this abbreviated protocol, the cohesion and internal friction of an asphalt concrete mixture could be determined using standard gyratory specimens without any further preparation and without the use of a triaxial cell or other specialized equipment.

2.3. Application of Triaxial Strength Testing and Mohr-Coulomb Failure Theory to Hot-Mix Asphalt Concrete

The most important early research involving triaxial testing of asphalt concrete mixtures was preformed by Nijboer and thoroughly documented in the text *Plasticity as a Factor in the Design of Dense Bituminous Road Carpets* (Nijboer, 1948). Nijboer describes the basic principal of the triaxial strength test and develops a comprehensive theory for explaining the behavior of bituminous materials during the triaxial test. Pertinent features of his theory are as follows:

- The cohesion of asphalt concrete, which Nijboer calls the initial resistance, is composed of three forces: true cohesion, apparent cohesion, and interlocking resistance.
- Bituminous mixtures, unlike soils, will exhibit a component of the cohesion called mass viscosity, which is proportional to the applied deviator stress and is also time dependent.
- Internal friction is that portion of the shear resistance proportional to the applied normal stress.
- The results of triaxial tests on asphalt concrete will depend on both loading rate and temperature.
- The value of ϕ determined under static (very slow) loading, termed the equilibrium value, is generally slightly higher than that determined at higher rates.
- Asphalt binders in general have a lubricating effect on aggregates, reducing the angle of internal friction.
- The stiffer the binder used in a mixture, the lower the angle of internal friction.

- The cohesion, and its two components (initial resistance and mass viscosity), all increase with increasing binder stiffness.
- Initial resistance, mass viscosity, and internal friction all decrease with increasing air void content.
- Increasing filler/binder ratio will increase both initial resistance and mass viscosity.
- Increasing the coarse aggregate content will normally increase all components of the shear resistance: initial resistance, mass viscosity, interlocking resistance, and internal friction.

Nijboer goes on to develop theoretical and semi-empirical relationship between these shear resistance parameters and mixture composition, eventually making specific recommendations concerning structural design of mixtures, including suggested aggregate gradations under different condition and preferred filler/binder ratios (Nijboer, 1948).

Hewitt developed a complete mixture design system based on shear strength, relying primarily upon triaxial strength testing and related analyses (Hewitt, 1964). Hewitt presents an equation for allowable surface contact pressure, based upon strength theories of soil mechanics. The version of this equation applicable to surface courses is given as:

$$p = \frac{4c}{1-\sin\phi}\left(\frac{1+\sin\phi}{1-\sin\phi}\right)^{0.5}, \tag{7}$$

where:

p = surface contact pressure;

c = cohesion (units consistent with p); and

ϕ = angle of internal friction.

The mixture cohesion and internal friction values can be determined through triaxial strength testing. Hewitt reported on the results of triaxial strength testing of several different mixtures under a wide range of conditions. In general, his findings supported Nijboer's work; the internal friction and cohesion were strongly dependent on both temperature and rate of loading. At higher temperatures, where rutting is a concern, Hewitt found that cohesion increased with decreasing temperature or increasing loading rate, while internal friction decreased with decreasing temperature or increasing loading rate. Similarly, pavement bearing

strength at high temperatures increased with increasing loading rate. Hewitt made a convincing case that mixture design, including determination of optimum binder content, could be rationally based upon triaxial testing and the analyses of the resulting data. The strong dependence of triaxial strength data and Mohr-Coulomb failure parameters on temperature and loading rate found by both Nijboer and Hewitt point out the importance of carefully selecting test conditions. This issue is discussed in some detail in the following section.

Huschek extended Nijboer's work in the plastic deformation of asphalt concrete mixtures (Huschek, 1985). He attempted to more precisely quantify Nijboer's model through extensive testing of several asphalt concrete mixtures under complex loading sequences. Although Huschek was able to qualitatively verify Nijboer's model, scatter in the data prevented a quantitative verification. Huschek concluded that the most important factors influencing the shear resistance of asphalt concrete mixtures were aggregate gradation, binder content, and binder consistency (Huschek, 1985).

Sebaaly and Krutz used triaxial testing in conjunction with repeated load testing to evaluate the resistance to permanent deformation of several asphalt concrete mixtures (Sebaaly and Krutz, 1993). This research was not as extensive as that of the previous researchers but did demonstrate the utility of the triaxial strength test in evaluating asphalt concrete mixtures. Of particular importance was the apparent relationship between strength tests and the results of repeated load testing, although this feature of the data was not emphasized or explored by the authors.

Based upon the work of these researchers, it is clear that the triaxial strength test and the Mohr-Coulomb failure parameters c and ϕ determined from these tests are potentially very useful tools for designing and evaluating asphalt concrete mixtures. This approach to mixture analysis is particularly useful for evaluating resistance to permanent deformation since the strength tests performed at high temperatures are strongly related to the resistance of the mixture to plastic shear deformation. Hewitt's suggestion of a bearing strength formula renders the approach potentially quantitative and rational. Furthermore, since this approach provides the engineer with information concerning both the internal friction and cohesion, it should be extremely useful in troubleshooting marginal mixtures.

The objectives of this work are to more clearly demonstrate the relationship between triaxial strength data and rut resistance by comparison of test data with field performance and with a well-accepted laboratory test for predicting rut resistance, the repeated shear at constant height

test (RSCH) run using the Superpave shear test (SST) device. A second objective is to render triaxial testing more practical by evaluating an abbreviated procedure which could be easily performed by any moderately proficient laboratory technician without using any specialized equipment. Additionally, the research team felt that further attention should be given to determining optimum test conditions for performing triaxial strength tests on asphalt concrete. This last issue is discussed in detail in the following section.

2.4. Determination of Appropriate Test Conditions for Strength Testing of Asphalt Concrete Mixtures

In order to establish correlations between pavement performance and triaxial strength data, and between the repeated shear test and strength data, it is essential to perform the strength tests at an appropriate temperature and loading rate. Traffic loading and the loading during the RSCH test occur relatively quickly but at high temperatures, the critical temperature for rutting in the Northeast typically being between 50° and 55 °C. Strength tests, on the other hand, are normally executed slowly to prevent uneven loading, transients, and dynamic effects. Compressive strength tests on portland cement concrete, for example, typically require between 30 seconds and 2 minutes to complete. The approach taken by the research team in developing appropriate test conditions was to approximately apply time-temperature superposition to determine a temperature and loading rates for the various strength tests used in this research. Test conditions were sought that would result in a failure time of about 20 seconds, and that would also rheologically approximate traffic loading time at the critical temperature for rutting. The discussion below presents this analysis.

A typical pavement section was analyzed under truck loading to determine the strain rate in the pavement. The assumed properties of the pavement were as follows:

- Thickness of asphalt concrete layer: 150 mm
- Thickness of crushed stone layer: 150 mm
- Modulus of asphalt concrete: 690 MPa
- Modulus of crushed stone, in lbf/in^2, given by $6{,}000\ \theta^{0.55}$ (typical values according to Kalcheff and Hicks, 1973)
- Modulus of subgrade, 55 MPa, typical for medium clay (Huang, p. 366)
- Poisson's ratio 0.35 for HMA and crushed stone, 0.40 for subgrade (Huang, p. 366)

- Tire type: dual wheel, single axle
- Tire radius, 100 mm, tire pressure, 690 kPa, tire spacing, 250 mm
- Stress point for non-linear calculation at 75 mm from top of crushed stone layer
- Stresses and strains calculated at 50-mm depth, below tire and between tires

Using Kenlayer, a program developed for layered elastic analysis of flexible pavements (Huang. 1993), the maximum vertical strain for this system occurs under the center of each tire and is 0.0053 (0.53 %). Huang cites Barksdale's study as indicating that for a truck traveling at 48 kph, at a pavement depth of 50 mm, the equivalent triangular pulse loading time is 0.06 s, meaning that 0.03 s is required to reach the maximum strain (Huang, 1993; Barksdale, 1971). Therefore, at a maximum compressive strain of 0.0053, the loading rate under these conditions would be $0.0053/0.03 = 0.18\ s^{-1}$. For a 150-mm-high gyratory specimen, this is equivalent to a loading rate of 1.6 m/min.

These loading conditions, meant to simulate loading as it occurs during rutting, would normally occur at elevated temperatures. In the case of Pennsylvania S.R. 11, the highway in which most of the mixtures to be used in this research were placed, the critical temperature would be 53°C, which is the maximum 7-day average high pavement temperature for Harrisburg, PA. In the laboratory, loading rates cannot be applied quickly enough to simulate traffic loading, and even if it were possible, the data would probably be unreliable due to transients and other errors inherent in dynamic loading; therefore, the testing must be done at a slower rate, but at a lower temperature, to maintain rheological equivalence during testing.

From Krutz and Sebaaly's research using triaxial tests (1994), failure strains of about 2 % can be expected for the confined and unconfined compressions tests. This represents a deflection of about 3 mm for a 150-mm-high specimen. To achieve a reasonable failure time of 20 seconds, a loading rate of 9.1 mm/min would be needed. The appropriate temperature can be found by application of time-temperature superposition. Christensen and Handojo (1999) have found a typical activation energy of 220 kJ/mol-°K for a variety of asphalt concrete mixtures. Applying the Arhennius equation using this value for activation energy results in a temperature of about 33°C at a 7.7 mm/min-loading rate as being equivalent to 53°C at a loading rate of 1.6 m/min; however, "ASTM D-1074: Standard Test Method for Compressive Strength of Bituminous Mixtures" calls for a loading rate of 0.05 mm/min per mm of specimen height. For a

150-mm specimen, this would result in a loading rate of 7.5 mm/min. In the interest of maintaining consistency with existing standards, 7.5 mm/min. is therefore the suggested loading rate for both confined and unconfined compressive strength tests to be performed as part of this project. Furthermore, it is suggested that as a tentative standard protocol, the triaxial strength, unconfined compression, and IDT test be performed at a temperature 20°C below $T_{eff(PD}$: 53 – 20 = 33°C in this case. The expected time of failure for these tests, based upon failure strains of 1% to 3 %, would then range from 12 to 36 seconds. In the case of the IDT test, the stresses of the loading rate must be adjusted, since the failure stress and strains are much less, although the indirect loading partly offsets this factor. Considering these factors, the research team selected a loading rate of 3.75 mm/min for the IDT test. This analysis assumes a Poisson's ratio of 0.5. Assuming failure strains similar to those in compression, the expected time to failure for the IDT test would also be 12 to 36 seconds. The specimen sizes, test temperature, and loading rates are summarized in Table 1.

Table 1. Specimen Size, Test Temperature, and Loading Rate.

Procedure	Nominal Specimen Size (mm)	Test Temp. (°C)	Loading Rate (mm/min)
Unconfined compressive strength	70 Dia. by 140 high	35	7.5
Confined (200 kPa) compressive strength	70 Dia. by 140 high	35	7.5
Unconfined compressive strength	150 Dia. by 150 high	35	7.5
Indirect tension	150 Dia. by 100 high	35	3.75

3. MATERIALS, METHODS, AND EXPERIMENT DESIGN

There were two groups of mixtures used in this research project: Six mixtures were based upon materials used in the S.R. 11 project in Pennsylvania (Fee, 1993; Ramirez, 1995), and four were based upon mixtures used in the New York Superpave implementation study (Anderson et. al., 1999). These mixtures were selected for a variety of reasons. The S.R. 11 mixtures were included because of the relatively thorough documentation of these materials, their performance in the field, and the range of aggregates and binder used. The N_{design} mixtures were included in order to evaluate the effect of level of N_{design} on the triaxial strength data and resulting Mohr-Coulomb failure parameters. These projects and the materials used during their construction are described in detail in the following sections of this report.

3.1. Pennsylvania Route 11 Study

This project was completed in October of 1991, the test section is located on S.R. 11 in Cumberland County, PA, between segment 0660/offset 2815 and segment 0680/offset 0704 (Ramirez, 1995). This section of pavement was receiving extremely heavy traffic, with a high proportion of trucks, and also included numerous intersections and traffic lights. The project involved an overlay of existing pavement, which was milled out to a depth of 100 mm to 125 mm. In the south end of the test section, the milling removed pavement down to the original portland cement concrete (PCC) material, but at the north end, there was still 75 mm to 100 mm of bituminous material remaining over the original PCC after milling. The overlays were all placed over 50 mm of ID-2 heavy-duty binder course material. A total of eight different test materials were included in this test section:

- ID-3 wearing course mixture with ethyl-vinyl acetate (EVA)-modified binder
- ID-2 wearing course mixture with EVA-modified binder
- ID-3 wearing course mixture with AC-40 binder
- ID-2 wearing course mixture with AC-40 binder
- ID-3 wearing course mixture with AC-20 binder
- ID-2 wearing course mixture with AC-20 binder
- ID-3 wearing course mixture with styrene-butadiene (SB)-modified binder
- ID-2 wearing course mixture with SB-modified binder

In other words, both ID-3 and ID-2 wearing course mixtures were used, with four different binder types, two unmodified and two modified with common commercial polymer modifiers. The ID-2 wearing course mixture was a Marshall heavy-duty mix design, using 9.5-mm nominal maximum-size aggregate. The ID-3 mixture was also a Marshall heavy-duty mix design but with a 19-mm nominal maximum-aggregate size. The two AC-40 mixtures were placed on the southbound passing lane, and the two AC-20 mixtures were placed in the northbound passing lane. The two EVA mixtures were placed in the southbound traffic lane, while the two SB mixtures were placed in the northbound traffic lane (Fee 1993; Ramirez 1995). Unfortunately, it was discovered after construction of the project that there were dramatic differences in the traffic level in the traffic and passing lanes. Traffic counts performed over a two day period in 1992 gave traffic levels of 2957 and 44 ESAL/day for the northbound travel and passing lanes, respectively, and 2653 and 114 ESAL/day for the southbound travel and passing lanes, respectively (Fee 1993; Ramirez 1995). Therefore, the mixtures made using the unmodified binders received much less traffic than the mixtures made using the modified binder. As discussed below, this makes interpretation of the rut depths somewhat complicated.

The Pennsylvania Department of Transportation measured rut depths in the test section over a four-year period following construction. The results are summarized in Table 2. Although there does not appear to be much difference in the performance of the binders, the reader should keep in mind that the mixtures made with the EVA- and SB-modified binders were subjected to from about 25 to 60 times as much traffic as were the mixtures made with the AC-40 and AC-20 binders. In figures 4 and 5, rut data for these eight mixtures have been plotted versus estimated traffic (on a semi-logarithmic scale). From these figures, it appears that the ID-2 mixtures in general performed slightly better than the ID-3 mixtures, with the exception of those containing the SB-modified binder, where the performance was reversed. This is somewhat surprising since the ID-3 mixture was developed by PennDOT to be more rut-resistance than the ID-2 wearing course mixture. Furthermore, the ranking of the binders from most rut resistance to least rut-resistant would be as follows:

1. EVA-modified binder
2. SB-modified binder (very close to EVA-modified)
3. AC-40
4. AC-20, especially when used in ID-3 wearing course mixture

In order to make direct comparisons with triaxial strength test data and related parameters, it is necessary to quantify the rutting rate with respect to traffic loading. This was done by performing linear regression on log-log transforms of rut depth versus traffic level (R^2 75 to 98 %). The resulting equations were used to estimate the rut depth for each mixture at a traffic level of 1,000,000 ESALs. These values are given in Table 3.

Table 2. Rut Depth (mm) Measurements for S.R. 11 Study.

	EVA		AC-40		AC-20		SB	
Year	**ID-3**	**ID-2**	**ID-3**	**ID-2**	**ID-3**	**ID-2**	**ID-3**	**ID-2**
1992	1.3	0.8	0.5	0.3	2.5	1.3	1.1	1.9
1993	1.7	1.3	1.1	0.8	2.6	2.1	1.8	2.2
1994	1.6	1.9	1.6	1.4	3.3	2.6	2.6	3.3
1995	2.4	1.7	1.9	1.4	4.0	2.8	3.1	3.8

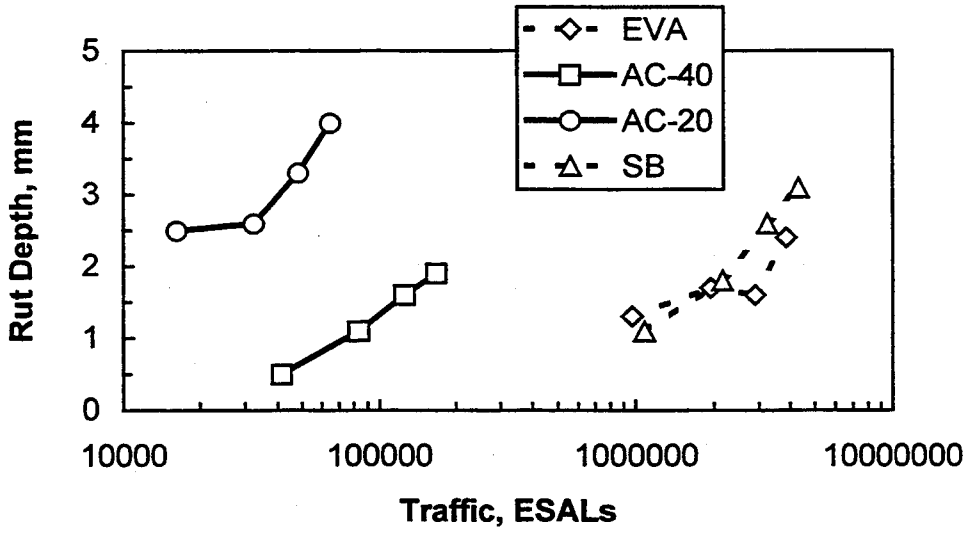

Figure 4. Rutting Data as a Function of Estimated ESALs for S.R. 11 ID-3 Mixtures.

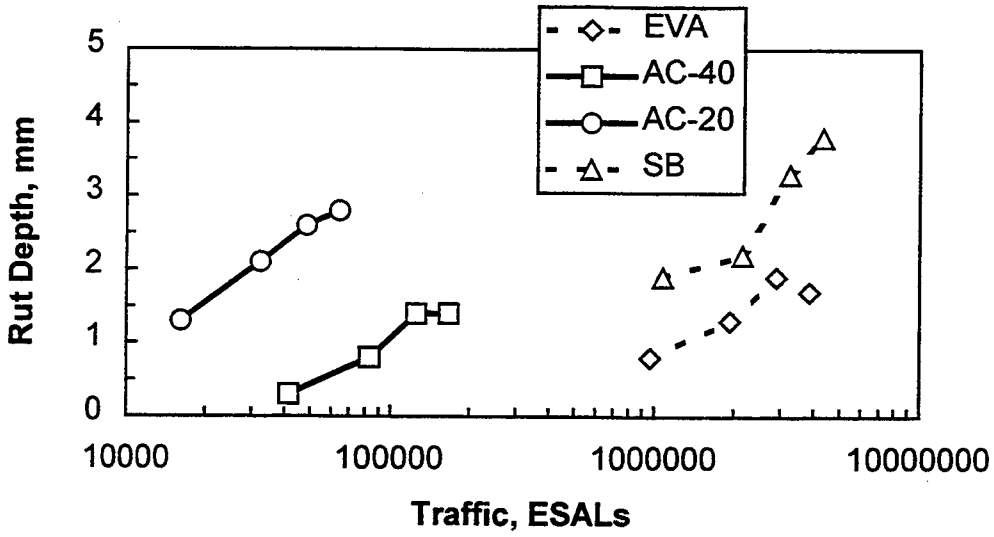

Figure 5. Rutting Data as a Function of Estimated ESALs for S.R. 11 ID-2 Mixtures.

Table 3. Estimated Rut Depths at 1,000,000 ESALs for S.R. 11 Mixtures.

	EVA		AC-40		AC-20		SB	
	ID-3	ID-2	ID-3	ID-2	ID-3	ID-2	ID-3	ID-2
Rut depth, mm:	1.3	0.9	11.8	13.9	9.2	14.0	1.0	1.7

Within a few months of construction of the S.R. 11 project, premature rutting was noted in several intersections outside the study area, which had been paved with the ID-3/AC-20 mixture. Cores were taken from these intersections to determine the reason for the poor performance, but the only unusual finding was relatively high mineral filler contents. For this reason, the research team felt it would be useful to include several mixtures based on the ID-3/AC-20 design, but with excess mineral filler, to determine if the triaxial test would be sensitive to these low-performance mixtures (Fee, 1993).

At the start of this research project, the research team selected six of the eight S.R. 11 mixtures for inclusion in this study: both ID-3 and ID-2 wearing course mixtures using the AC-20, EVA-modified, and SB-modified binders. In addition, two ID-3/AC-20 mixtures were included with excess mineral filler—one with 1 % excess (ID3/AC20/MF+), and one with 2 % excess mineral filler (ID3/AC20/MF++). Suppliers of the original binders and aggregates were contacted and agreed to supply either the same material as was used for these mixtures or a reasonably close substitute; however, the supplier of the EVA-modified binder did not supply

this binder, so only six mixtures from the S.R. 11 project were included in this study. The sections below describe the designs of these mixtures and the pertinent properties of their constituent materials.

3.2. S.R. 11 Mix Designs

The ID-2 and ID-3 mixtures were 75 below Marshall designs and were produced using sandstone coarse aggregate and limestone fine aggregate. Table 4 is a summary of mixture design data obtained from the contractor's project submittal. For preparation of the laboratory mixtures, samples of aggregates were obtained from the quarries used during the field project.

Table 4. Mixture Design Data for S.R. 11 Mixtures.

Property	ID-2	ID-3
Size:	*Percent Passing*	
25 mm	100	100
19 mm	100	93
12.5 mm	100	---
9.5 mm	93	72
4.75 mm	64	50
2.36 mm	43	36
1.18 mm	25	21
0.600 mm	15	12
0.300 mm	9	8
0.150 mm	6	6
0.075 mm	4.5	4.5
Asphalt Content, %	6.3	5.1
Stability, lbs.	3225	3864
Flow, 1/100 in	11.2	11.7
Air Voids, percent	3.9	4.0
VMA, percent	15.9	13.5
VFA, percent	75.5	70.5

A substantial amount of quality control data for these mixtures were obtained from Mr. Roger Studer of Hempt Bros., Inc. This data included the results of asphalt content, gradation, and theoretical maximum specific gravity tests performed on the plant produced mixtures. The data included 22 observations for the ID-2 and 85 observations for the ID-3 mixtures; recall that the ID-3 mixture was also used in the paving that occurred beyond the intersection study area. The averages from the quality control data were used to establish the gradation and asphalt

contents for the laboratory-prepared specimens. These are summarized in Table 5 and presented in figures 6 and 7. The ID-2 mixture meets the gradation requirements of a Superpave 9.5-mm nominal-size mixture. The ID-3 meets the gradation requirements of a Superpave 19.0-mm nominal-size mixture, but it enters the restricted zone between the 1.18- and 2.36-mm sieves.

Table 5. Composition of S.R. 11 Laboratory Mixtures.

	ID-2		ID-3		ID-3 MF+	ID-3 MF++
Property	**QC**	**Lab**	**QC**	**Lab**	**Lab**	**Lab**
Size	*Percent Passing*					
25 mm	100	100	100	100	100	100
19 mm	100	100	95	95	95	95
12.5 mm	100	100	78	78	78	78
9.5 mm	96	96	68	68	68	68
4.75 mm	62	62	52	52	52	52
2.36 mm	42	42	36	36	37	37
1.18 mm	24	25	21	21	22	22
0.600 mm	15	15	13	12	14	14
0.300 mm	9	9	8	8	9	9
0.150 mm	6	5	5	5	6	7
0.075 mm	3.8	3.8	3.8	3.8	4.8	5.8
Asphalt Content, %	6.0	6.1	4.8	4.9	4.9	4.9

3.3. S.R. 11 Binders

Samples of the binders used in the construction of the test sections were not available in sufficient quantities for this study. Koch Materials Company, which supplied binders during the original construction of the project, provided an unmodified PG64-22 and laboratory-blended SB-modified binder that were similar to the binders used during construction. The PG-grade of the SB-modified binder was PG 76-28. Table 6 summarizes AASHTO MP1 grading data for the binders used in this study. The modified binder was produced in approximately 8-gallon batches in the laboratory. Table 6 includes test results for both batches, and Table 7 presents recommended laboratory mixing and compaction temperatures for the two binders.

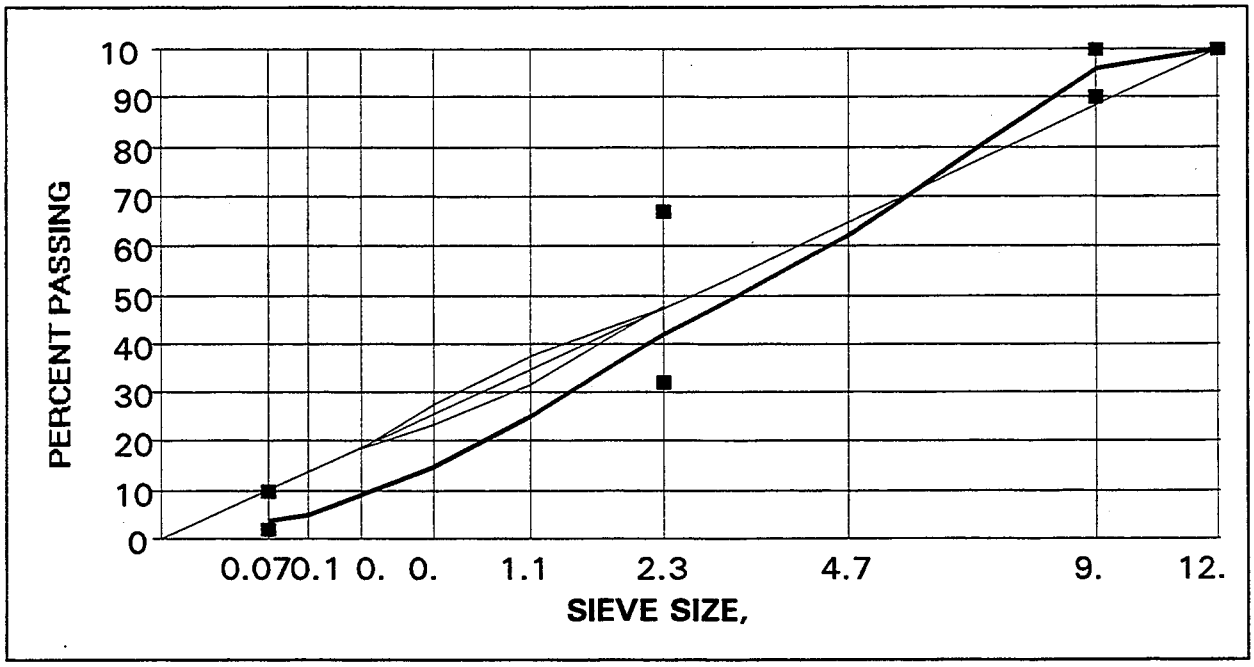

Figure 6. Aggregate Gradation for S.R. 11 ID-2 Mixtures.

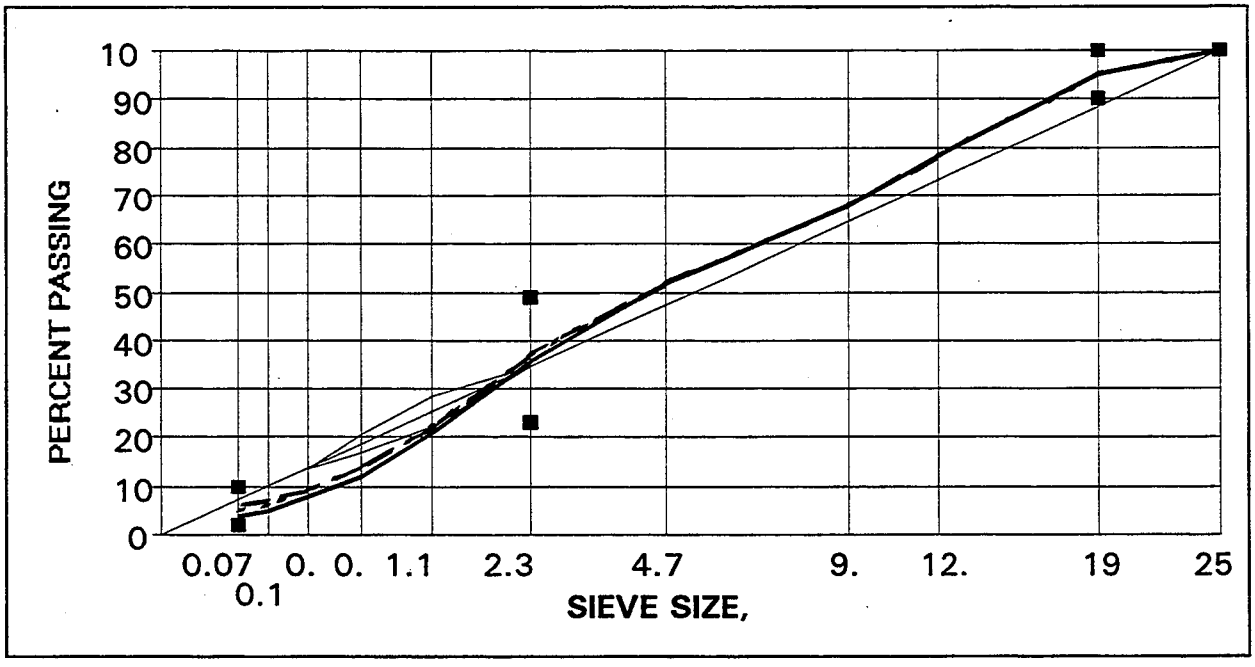

Figure 7. Aggregate Gradation for S.R. 11 ID-3 Mixtures.

Table 6. AASHTO MP1 Grading for S.R. 11 Binders.

Test	Method	PG 64-22	PG 76-28	
			Blend A	Blend B
	Unaged Binder			
Specific Gravity at 25 °C	AASHTO T228	1.032	1.027	1.027
Flash Point, °C	AASHTO T48	285	302	302
Viscosity at 135 °C, Pa-s	ASTM D4402	0.47	2.38	2.33
G*/sin δ, at 10 rad/sec and 64 or 76 °C, kPa	AASHTO TP5	1.29	1.61	1.63
	RTFOT Residue			
Mass Change, %	AASHTO T240	-0.359	-0.359	-0.306
G*/sin δ, at 10 rad/sec and 64 or 76 °C, kPa	AASHTO TP5	3.876	3.87	4.14
	PAV Residue			
G* × sin δ, at 10 rad/sec and 25 °C, kPa	AASHTO TP5	1010	1010	1380
Creep Stiffness, at 60 sec and –12 or –18 °C, MPa	AASHTO TP1	157	157	176
m-value at 60 sec and –12 or –18 °C	AASHTO TP1	0.318	0.318	0.312

Table 7. Mixing and Compaction Temperatures for S.R. 11 Binders.

Binder	Condition	Temperature, °C	
		Maximum	Minimum
PG 64-22	Mixing	160	156
	Compaction	147	143
PG 76-28	Mixing	163	154
	Compaction	157	149

3.4. New York N_{design} Study

Four Superpave 12.5-mm nominal size mixtures from a Superpave implementation study performed by the New York Department of Transportation were also included in the study (Anderson et. al., 1999). These mixtures were a subset of field projects designed for various traffic levels which are being monitored over time by the New York State DOT. Table 8 summarizes the field projects that were selected for this study. The research team included these mixtures to evaluate the effect of changes in N_{design} on mixture cohesion and internal friction. The reader should keep in mind that these mixes used different aggregate sources and two different binders. The value of N_{design} varied from 76 to 126, but the binder content and other volumetric parameters remained more or less constant.

Table 8. New York N_{design} Projects.

Project	Design Traffic	N_{design}	Binder	Year
Route 316	< 1.0 Million ESAL	76	PG 58-28	1997
Route 12	< 10.0 Million ESAL	96	PG 58-28	1998
Interstate 81	< 30.0 Million ESAL	109	PG 64-28	1997
Interstate 81	< 100.0 Million ESAL	126	PG 64-28	1997

3.5. Design of the New York N_{design} Mixtures

Each of the New York mixtures was designed by the paving contractors, using the Superpave volumetric mixture design method. Table 9 summarizes pertinent design properties for three of these mixtures obtained from the project job mix formulas; JMF data for the 126-gyration design was not provided to the research team. Quality control data was not available for the New York mixtures. The laboratory specimens were prepared based on the job mix formulas using source aggregate samples supplied by the New York State DOT Materials Bureau. For I-81 mixtures, the job mix formula asphalt content was reduced based on changes made during field production. Table 10 compares gradations from the job mix formulas and the laboratory blends. The laboratory gradations are shown graphically in Figure 8. All mixtures have gradations below the restricted zone, with the I-81 gradations being somewhat coarser.

Table 9. Design Properties for New York N_{design} Mixtures.

Property	Route 316	Route 12	I-81 (109)	I-81 (126)
Size	*% Passing*			
19.0 mm	100	100	100	100
12.5 mm	100	100	98	99
9.5 mm	88	90	87	90
4.75 mm	55	53	47	46
2.36 mm	34	32	28	28
1.18 mm	22	20	19	15
0.600 mm	13	13	12	10
0.300 mm	8	8	9	7
0.150 mm	5	5	5	5
0.075 mm	4.0	2.6	3.7	4
Asphalt Content, %	5.1	5.1	5.6	5.6
Binder Grade	PG 58-28	PG 58-28	PG 64-28	PG 64-28
N_{design}	76	96	109	126
Air Voids, %	4.0	3.8	4.0	---
VMA, %	14.5	14.8	15.2	---
VFA, %	72.5	74.6	72.8	---
Filler/Effective Asphalt Ratio	0.7	0.6	0.8	---
% G_{mm} at $N_{initial}$	84.7	84.8	84.2	---
% G_{mm} at $N_{maximum}$	97.7	97.8	97.6	---
Coarse Aggregate Angularity	100/100	100/100	96/92	---
Fine Aggregate Angularity	45.7	48.3	46.4	---
Flat and Elongated	1.0	0.1	0.3	---
Sand Equivalent	66.9	58.0	67.8	---

Table 10. Laboratory Gradations for New York N_{design} Mixtures.

Property	Route 316		Route 12		I-81 (109)		I-81 (126)	
Property	**JMF**	**Lab**	**JMF**	**Lab**	**JMF**	**Lab**	**JMF**	**Lab**
Size	*Percent Passing*							
19.0 mm	100	100	100	100	100	100	100	100
12.5 mm	100	100	100	100	98	99	99	99
9.5 mm	88	88	90	90	87	87	90	90
4.75 mm	55	55	53	53	47	47	46	46
2.36 mm	34	32	32	32	28	28	28	28
1.18 mm	22	23	20	20	19	19	15	18
0.600 mm	13	15	13	12	12	13	10	11
0.300 mm	8	8	8	7	9	8	7	7
0.150 mm	5	5	5	5	5	5	5	5
0.075 mm	4.0	4.0	2.6	3.2	3.7	3.9	4.0	3.9
Asphalt Content %	5.1	5.1	5.1	5.1	5.6	5.5	5.6	5.5

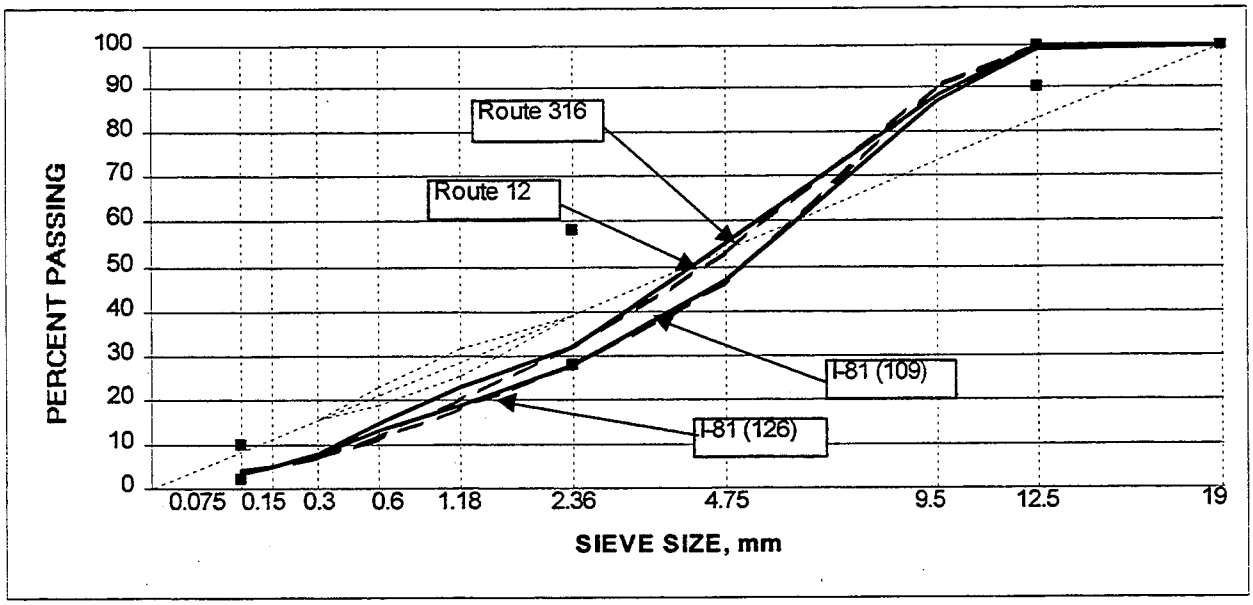

Figure 8. Laboratory Gradations of New York N_{design} Mixtures

3.6. New York N_{design} Binders

Samples of binders of the same grade as those used in construction were obtained from the suppliers. A PG 58-28 binder was used for the Route 316 and Route 12 projects, and a PG 64-28 binder was used for the two I-81 projects. Table 11 is a summary of the PG binder grading test data for these two binders. Table 12 presents recommended laboratory mixing and compaction temperatures for the two binders.

Table 11. AASHTO MP1 Grading for New York Binders.

Test	Method	PG 58-28	PG 64-28
Unaged Binder			
Specific Gravity at 25 °C	AASHTO T228	1.023	1.021
Flash Point, °C	AASHTO T48	270	> 230
Viscosity at 135 °C, Pa-s	ASTM D4402	0.337	2.96
G*/sin δ, at 10 rad/sec and 58 or 64 °C, kPa	AASHTO TP5	1.78	1.73
RTFOT Residue			
Mass Change, %	AASHTO T240	-0.59	-0.01
G*/sin δ, at 10 rad/sec and 58 or 64 °C, kPa	AASHTO TP5	3.94	2.58
PAV Residue			
G* × sin δ, at 10 rad/sec and 25 °C, kPa	AASHTO TP5	3090	2200
Creep Stiffness, at 60 sec and –18 °C, MPa	AASHTO TP1	184	264
m-value at 60 sec and –18 °C	AASHTO TP1	0.383	0.335

Table 12. Mixing and Compaction Temperatures for New York N_{design} Binders.

Binder	Condition	Temperature, °C	
		Maximum	Minimum
PG 58-28	Mixing	149	143
	Compaction	137	132
PG 64-28	Mixing	157	152
	Compaction	143	138

3.7. Specimen Preparation

The experimental design required specimen of various sizes. Table 13 presents the various specimen sizes that were required. All specimens were prepared using an Interlaken gyratory compactor meeting the equipment requirements of AASHTO TP4. The triaxial strength and the repeated shear specimens were cored and sawed from larger gyratory specimen. The triaxial specimens were cored from the center of the gyratory specimen using a standard electric coring drill. A special stand was fabricated to hold the drill and specimen in alignment during coring. A double-bladed saw was used with both the triaxial strength and repeated shear specimen to ensure parallel specimen ends. The compressive strength and indirect tensile strength tests used specimens directly from the gyratory compactor. The target air void contents for the final test specimens was 4.0 % with a tolerance of ± 0.5 %. Air void contents for each of the final test specimens are included in the Appendix of this report, which is a table summarizing all project data.

Table 13. Summary of Required Specimen Sizes.

Test	Specimen Size		Superpave Gyratory
	Diameter, mm	Height, mm	Height, mm
Triaxial Strength	70	140	155
Repeated Shear	150	50	100 or 155
Compressive Strength	150	150	150
Indirect Tensile Strength	150	100	100

The gyratory specimens were prepared in accordance with AASHTO TP4, except the mass of the batches was adjusted to obtain specimens with the heights listed in Table 13. After mixing, the material was short-term oven-aged in accordance with AASHTO PP2 at a temperature of 135 °C for 4 hours. The mixtures required different levels of compactive effort to

produce specimens within the specified air void tolerances. Representative numbers of gyrations for each mixture are summarized in Table 14.

Table 14. Representative Number of Gyrations for Specimen Preparation.

Mixture	Number of Gyrations	
	100 mm High	150 and 155 mm High
ID-2, SB	300	1000
ID-3, SB	100	300
ID-2, AC-20	200	1000
ID-3, AC-20	100	200
ID-3, AC-20 +MF	100	200
ID-3, AC-20 ++ MF	50	100
Route 316, N_{design} 76	100	300
Route 12, N_{design} 96	500	1000
I-81, N_{design} 109	100	200
I-81, N_{design} 126	200	400

3.8. Test Procedures

The triaxial strength tests were performed on an MTS servo-hydraulic testing system. The tests were performed using a standard soil triaxial test cell for 70-mm-diameter specimen, purchased from a commercial laboratory supplies vendor. The tests were run unconfined and with 207 kPa confining pressure; the loading rate used was 7.5 mm/min, and all tests were preformed at 33 °C.

The tests using the abbreviated protocol were also performed on the MTS servo-hydraulic system. The compressive strength tests were performed directly on 150-by-150-mm gyratory specimens. The specimens were capped using reusable capping sets as used in testing portland cement concrete cylinders (ASTM C 1231, AASHTO T22). This system consists of two steel retainers, each containing a Neoprene pad. The system was modified by using 40-durometer neoprene, which is somewhat softer than the 50-durometer generally used for testing ordinary portland cement concrete. The systems can be purchased from commercial suppliers, but the 40-durometer pads were custom machined. These tests were performed using a loading rate of 7.5 mm/min at a temperature of 33 °C. The indirect tension test was also performed on the MTS system. All tests were performed on standard gyratory specimen, 100 by 150 mm. A standard

Lottman breaking head for 150-mm diameter specimen was used (ASTM D 4123, AASHTO T283). The loading rate was 3.75 mm/min, and the test temperature was again 33 °C.

The repeated shear-at-constant-height (RSCH) test was performed on an Interlaken Superpave Shear Test system according to procedures described in AASHTO TP7-94. A standard specimen size was used of 50 mm thick by 150 mm diameter. The test was run at the maximum 7-day average pavement temperature for south central Pennsylvania, 53 °C.

3.9. Experiment Design

The first experiment comprising this research involved determination of the Mohr-Coulomb failure parameters c and ϕ, which was done using two alternate approaches. The standard approach involved using unconfined and confined compressive strength tests on 70-by-140-mm cores and using these data in the subsequent analysis. The second approach consisted of testing 150-by-150-mm gyratory specimen in compression and 100-by-150-mm gyratory specimens in indirect tension. As discussed previously, determination of c and ϕ from either set of data involves three steps:

1. calculating p and q values using equations 2 and 3, respectively, for each specimen tested;
2. using linear regression to determine the intercept and slope of the K_f-line through the resulting points; and
3. calculating c and ϕ using equations 4 and 5, respectively, from the slope and intercept of the K_f-line.

In calculating p and q values from the indirect tensile strength test, a Poisson's ratio of 0.5 was assumed, resulting in $\sigma_1 = -3\sigma_3$. In analyzing these data, multiple regression approach was used, which involved setting up a series of indicator variables for each of the ten mixtures (Neter et. al., 1985). This allowed estimation of the standard deviation of the parameter estimates for each mixture and statistical comparisons. The resulting regression model is given by equation 8:

$$Y_i = \beta_0 + \beta_1 X_{i1} + \beta_2 X_{i2} + \beta_3 X_{i3} + \ldots + \beta_{10} X_{i10} + \beta_{11} X_{i1} X_{i2} + \beta_{12} X_{i1} X_{i3} + \ldots + \beta_{19} X_{i1} X_{i10} + \varepsilon_i \quad (8)$$

where:

Y_i = the measured values of q for the i^{th} observation;

β_0 = the intercept of the regression line for mixture 1;

β_1 = the slope of the regression line for mixture 1;

X_{i1} = the measured values of p for the i^{th} observation;

β_2 = difference between intercept values for mixture 2 and mixture 1;

X_{i2} = indicator variable for mixture 2;

β_3 = difference between intercept values for mixture 3 and mixture 1;

X_{i3} = indicator variable for mixture 3;

β_{10} = difference between intercept values for mixture 10 and mixture 1;

X_{i10} = indicator variable for mixture 10;

β_{11} = difference between slope values for mixture 2 and mixture 1;

β_{12} = difference between slope values for mixture 3 and mixture 1;

β_{19} = difference between slope values for mixture 10 and mixture 1; and

ε_i = error for the i^{th} observation.

For the standard test procedure, four replicate specimens were tested in almost every case, resulting in a total of about 80 tests. The number of replicates used for the abbreviated protocol testing varied from 2 to 4; the total number of tests run using this approach was 60. Since the model above has 20 parameters, the degrees of freedom for error is about 60 for the standard test method and 40 for the data using the abbreviated protocol.

The Mohr-Coulomb failure parameters as determined from the strength data were used for two primary purposes. The first was to determine if the triaxial strength test is an effective and simple means of evaluating the rut resistance of asphalt concrete mixtures. The second was to evaluate an abbreviated protocol for determining the triaxial strength parameters. Ideally, achieving the first objective could best be performed by comparing the results of triaxial strength tests with observed rutting rates in the field for a variety of mixtures under a range of traffic loading and a variety of environmental conditions. As discussed previously, the S.R.11 project was selected for inclusion in this study because of the range of materials used and the documented difference in observed rutting. Reliable measurements of rutting rates were available for four of the mixtures used on this project: the ID2 and ID3 mixtures, made with SB-modified PG76-22 binder and with an AC20 (PG 64-22) binder. There is anecdotal evidence concerning the field performance of the remaining two S.R. 11 mixtures, the ID3/AC20 mixtures

containing excessive mineral filler. These S.R.11 mixtures formed the basis for the comparison of triaxial strength data with observed rut resistance.

The 4 New York N_{design} mixtures were included primarily to evaluate the effect of design compaction level on the triaxial strength parameters. The research team believed that any simple performance test, to be useful in evaluating mixtures, should be sensitive to compaction level. In this case, there was special interest in the way in which changes in N_{design} would alter the internal friction and cohesion of the New York mixtures.

Because of this limited field data, the repeated shear test at constant height (RSCH) test was performed on all mixtures. This test, performed on the Superpave shear test (SST) device, has become an accepted standard for evaluating the rut-resistance of asphalt concrete mixtures in the laboratory; therefore, there were four separate but related experiments for performing the initial evaluation of the triaxial strength test:

1. Comparison of triaxial strength data with measured rut rates for the four primary S.R.11 mixtures;
2. Comparison of triaxial strength data with anecdotal evidence concerning the field performance of the ID3/AC20 mixture used on S.R.11 made using excess mineral filler;
3. Comparison of triaxial strength data with compaction effort (number of gyrations) for the four New York mixtures; and
4. Comparison of triaxial strength data with RSCH data for all ten mixtures.

The abbreviated protocol for determining Mohr-Coulomb failure parameters, as described previously, involved direct testing of gyratory specimens. The results of these tests can be used to determine Mohr-Coulomb failure parameters for comparison with those determined using 70-by-140-mm cores. In evaluating the abbreviated protocol for determining triaxial strength parameters, four primary experiments were used:

1. Comparison of unconfined compressive strength data gathered using the two methods
2. Comparison of angle of internal friction values
3. Comparison of cohesion values
4. Comparison of various other parameters related to Mohr-Coulomb fair theory as determined using the two techniques.

In general, four replicate tests were performed for each strength test: unconfined compression, confined (triaxial) compression, and split tension. For the repeated shear test, only two replicates were performed. The general statistical approaches used in comparing the various parameters involved analysis of variance and simple linear regression. In the latter case, the primary parameter of interest was the coefficient of determination, R^2, which indicates the degree of variability explained by the model. An R^2 value of 95 %, for example, indicates that the values of one variable can be used to predict 95 % of the variability in the second variable. In some cases, confidence intervals for regression parameters were considered in comparing values, along with simple plots for visual comparisons.

An important aspect of the analysis of any data on asphalt concrete mixtures is the effect of air voids on the measured properties. In this case, the air void content of all specimens was controlled to within ±0.5 %. Additionally, an attempt was made when selecting specimens for one test or another to balance out high and low air void specimens; however, to ensure that variation in air voids would not cause a spurious relationship to occur, and also to minimize error terms in all statistical analysis, an analysis of variance was run to quantify the effect of air voids on the measured strengths.

The final experiment comprising this study involved an evaluation of the need for using latex membranes during confined compression tests on asphalt concrete. Some researchers feel that because of the low permeability of dense-graded asphalt mixtures, latex membranes need not be used in performing confined compression tests. One of the graduate students performing the experimental work on this project had previous experience performing triaxial tests on asphalt concrete mixtures and routinely performed them without latex membranes; therefore, he performed confined compression tests on several mixtures without latex. Other research team members were not comfortable performing confined tests without membranes, and when his technique was observed, he was asked to perform half the remaining confined tests with latex membranes and half without. This comprised another experiment performed during the project, the objective being to determine if using latex membranes on dense-graded asphalt concrete mixtures was necessary when performing confined compression tests.

The primary experiments included in this project are summarized below in Table 15. Note that there are a total of 10 experiments listed. Of these, the most significant to the outcome of this research are the comparison of triaxial strength data with RSCH data and the comparison of

compressive strength and Mohr-Coulomb failure parameters found using the standard triaxial test approach with those found using the abbreviated protocol.

Table 15. Summary of Experiment Designs

Description	Statistical Approach	Statistical Design	Primary Results
Evaluation of effect of latex membrane on confined strength	Analysis of variance with air as covariate	Mixture x 6 levels Membrane x 2 levels Air as covariate 4 replicates	Level of significance for membrane
Evaluation of effect of air voids on strength data	Analysis of variance with air as covariate	Mixture x 10 levels Confinement x 2 levels Air as covariate 4 replicates	Factor for estimating effect of air on strength
Determination of c and ϕ from unconfined and confined compressive strength tests on 70 by 140 mm cores	Linear regression	Multiple regression with indicator variables for mixture	C and ϕ values and related statistics for each of 10 mixtures.
Determination of c and ϕ from unconfined compression and IDT tests on gyratory specimens	Linear regression	Multiple regression with indicator variables for mixture	C and ϕ values and related statistics for each of 10 mixtures.
Comparison of c and ϕ values as determined by testing 70 by 140 mm cores and as determined through testing of gyratory specimens	Graphical comparison	N/A	Subjective comparison of values
Comparison of unconfined compressive strength as determined using 70 by 140 mm cores and by using 150 by 150 mm gyratory specimens	Regression analysis and graphical comparison	Linear regression	R^2; comparison with line of equality
Evaluation of effect of changes in compactive effort on c and ϕ	Direct comparison	N/A	N/A
Comparison of strength data and c and ϕ with measured rut rates for SR11 primary mixtures	Graphical comparisons and linear regression analysis	4 observations 2 d.f. for error	Subjective evaluation of data; R^2
Comparison of strength data and c and ϕ with anecdotal evidence of field performance for SR11 ID3/AC20 mixtures containing excess mineral filler	N/A	N/A	Subjective
Comparison of strength data and c and ϕ with RSCH data for all 10 study mixtures	Linear regression analysis	10 observations 8 d.f. for error	R^2

4. RESULTS

The results of the unconfined and confined compressive strength tests on 70- by 40-mm cores are given in Table 16. The strength results for the abbreviated protocol using 150-by-50-mm gyratory specimens for compressive strength and 100- by-150-mm gyratory specimens for indirect tensile strength are summarized in Table 17. The repeated shear at constant height data is summarized in Table 18. A complete listing of individual data is included as an appendix to this report.

Table 16. Triaxial Strength Data Using 70 by 140 mm Cores.

Mixture	Compressive Strength, MPa	
	Unconfined	Confined
ID-2, SB	3.61	4.00
ID-3, SB	3.41	4.14
ID-2, AC-20	3.23	3.78
ID-3, AC-20	2.96	3.36
ID-3, AC-20 +MF	2.91	3.43
ID-3, AC-20 ++ MF	2.97	3.32
Route 316, N_{design} 76	1.79	2.45
Route 12, N_{design} 96	2.38	3.10
I-81, N_{design} 109	2.00	2.34
I-81, N_{design} 126	2.22	2.80

Table 17. Strength Data Using Abbreviated Protocol.

Mixture	Compressive Strength, MPa	IDT Strength, kPa
ID-2, SB	3.37	462
ID-3, SB	3.15	483
ID-2, AC-20	2.66	386
ID-3, AC-20	2.36	393
ID-3, AC-20 +MF	2.44	400
ID-3, AC-20 ++ MF	2.06	311
Route 316, N_{design} 76	1.72	200
Route 12, N_{design} 96	2.03	262
I-81, N_{design} 109	2.29	255
I-81, N_{design} 126	2.41	290

Table 18. Repeated Shear at Constant Height Test Data.

Mixture	Maximum Permanent Shear Strain, %
ID-2, SB	1.05
ID-3, SB	.65
ID-2, AC-20	1.72
ID-3, AC-20	1.13
ID-3, AC-20 +MF	.98
ID-3, AC-20 ++ MF	1.14
Route 316, N_{design} 76	2.84
Route 12, N_{design} 96	2.37
I-81, N_{design} 109	2.89
I-81, N_{design} 126	2.20

5. ANALYSIS

As described previously, this project involved a number of related experiments. Wherever possible, simple and appropriate statistical methods have been used to analyze the data, with special attention given to both the statistical and practical significance of the various factors. Analyses of the various experiments are presented and discussed in the following sections.

5.1. Effect of Membrane Usage for Confined Tests

An analysis of variance was performed on q-values ($q = (\sigma_1-\sigma_3)/2$)) to determine whether using a latex membrane for the confined tests had an effect on the resulting failure stress. In this case, only confined data was used and only for those mixtures in which both methods were used for confinement. Mixture type was used as a factor (6 levels), along with membrane (2 levels) and the interaction of mixture type and membrane. The air void content was used as a covariate in order to reduce the error term. The results of this analysis are summarized in Table 19. The P-values for both membrane and the interaction of mixture type and membrane are quite high, indicating that using (or not using) a latex membrane for the confined tests did not affect the strength of the specimens. This factor can therefore be ignored for the remaining analyses. The research team does not, however, believe that latex membranes need not be used in performing confined triaxial tests. In this case, because of the dense mixtures, relatively low air void content, and low confining pressures, the use of latex membranes was not needed, but in general, latex membranes should be used for confined tests. This is especially important if open-graded mixtures are used or the air void content of some of the specimen is high, and/or the confining pressure is high.

Table 19. Analysis of Variance of Effect of Membrane on Confined Tests.

Source	DF	Seq SS	Adj SS	Adj MS	F	P
Air Voids	1	4019.1	418.2	418.2	4.59	0.055
Mixture Type	5	18542.4	18597.9	3719.6	40.84	0.000
Membrane	1	163.1	76.3	76.3	0.84	0.380
Type*membrane	5	473.9	473.9	94.8	1.04	0.441
Error	11	1001.8	1001.8	91.1	---	---
Total	23	24200.4	---	---	---	---

5.2. Effect of Air Void Content on Triaxial Strength Data

An analysis of variance was done to determine the effect of air voids on triaxial strength data. The dependent variable in this case was $p = (\sigma_1+\sigma_3)/2$, although as pointed out below, either p or q can be used with essentially identical results. In this case, all mixtures were included in the analysis, resulting in 10 levels for mixture type. Confinement (unconfined vs. confined) was also used as a factor, with 2 levels, along with the interaction of mixture type and confinement. The level of air voids was included as a covariate. The results are summarized in Table 20. Note the high levels of significance (P=0.001, 0.000, 0.000) for air voids, mixture type, and confinement. The interaction of mixture type and confinement was not significant in this case, indicating that statistically confinement had a similar effect on all mixtures.

Table 20. Analysis of Variance for Effect of Air Voids on Triaxial Strength.

Source	DF	Seq SS	Adj SS	Adj MS	F	P
Air Voids	1	2931	2145	2145	12.82	0.001
Mix Type	9	140769	140305	15589	93.21	0.000
Confinement	1	55630	54868	54868	328.06	0.000
Type × confinement	9	1576	1576	175	1.05	0.415
Error	57	9533	9533	167	---	---
Total	77	210440	---	---	---	---

The coefficient found for air voids was in this case –0.159, indicating that the value of p decreases by 0.159 MPa for every 1-% increase in air voids. A corresponding analysis was done using $q = (\sigma_1-\sigma_3)/2$ as the dependent variable to verify the results of the analysis on p-values. The results showed an identical effect on q of air voids. Because of the significant dependence of p and q values on air voids, p and q values were normalized to account for this effect, by calculating the equivalent value at 4 percent air voids, assuming that they would decrease by 0.159 MPa for each 1 % increase in air voids. Subsequent analyses were generally done using both raw and normalized values of p and q. Although little difference was found in absolute terms using these two approaches, in general, the statistical analyses were better when using data normalized with respect to air voids; therefore, the analyses presented in the remainder of this report involving standard triaxial strength data are all based upon such normalized data.

5.3. Determination of c- and ϕ- Values

A multiple regression analysis was run to determine the intercepts and slopes of the functions relating q- and p-values for strength data from both the standard triaxial tests and the abbreviated protocol. The results for the standard method are summarized in Table 21(a) below, and the results for the abbreviated protocol are summarized in Table 21(b); the associated analysis of variance is summarized in Table 21(c). Note that in tables 21(a) and 21(b),the intercept coefficients are in units of kPa and the slopes given as gradients. The rather complicated model was described previously (Equation 8) under *Experiment Design*. Care must be taken in interpreting the results of this analysis; the coefficients given for the indicator variables represent the difference relative to the common slope and intercept, which in this case are for the ID2/AC20 control mixture used on S.R. 11, as determined using the standard triaxial testing method. Furthermore, the T- and P-values similarly refer to the significance of a given indicator variable compared to the common slope and intercept. In other words, low significance levels only indicate that the response for the given mixture was statistically similar to that of the control mixture and test method and not necessarily that the response of the mixture was similar to all other mixtures.

In general, the standard deviations for the parameters are quite high, indicating a high degree of variability in the data; however, the research team believes that the statistical analysis overestimates the variability in this analysis. Changes in asphalt concrete composition, including not only air voids but asphalt content, mineral filler content, and distribution of large aggregate particles, will tend to affect unconfined and confined strength in a similar manner. The regression analysis, however, assumes that the association between unconfined and confined test results is completely random and that a high value for confined compressive strength has an equal chance of being associated with any of the measured unconfined responses—even the lowest. This overestimation of variability is difficult to quantify, but support for its existence can be found in the various analyses presented below, where very good correlations are found between these parameters and other data. If the variability were truly as high as indicated by the statistics, then such correlations would not be likely. Further work should be done in developing specimen preparation and testing protocols to minimize this problem.

The actual values for c and ϕ were determined from the slope and intercepts of the regression lines, using equations 2 through 5 given previously. These values are listed in Table

22. Also listed in this table are values of bearing strength, calculated according to Hewitt's method, using Equation 7. Further analyses and comparisons are presented in the following sections.

Table 21(a). Summary of Regression Analysis for Determination of *c*- and ϕ-Values for Standard Triaxial Tests (r^2, Adj. = 99.1 %).

Predictor	Coef.	St. Dev.	T	P
Intercept (ID2/AC20)	721.2	114.8	6.28	0.000
Slope (ID2/AC20)	0.55262	0.06187	8.93	0.000
Indicator variables for difference in intercept				
ID3/AC20	138.0	180.6	0.76	0.446
ID2/SB	13.7	174.2	0.08	0.938
ID3/SB	-14.3	160.0	-0.09	0.929
ID3/AC20/MF+	80.7	164.6	0.49	0.625
ID3/AC20/MF++	84.7	181.0	0.47	0.641
NY76	-347.7	132.2	-2.63	0.010
NY96	-245.4	139.5	-1.76	0.081
NY109	-69.5	157.7	-0.44	0.660
NY126	-218.0	142.2	-1.53	0.128
Indicator variables for difference in slope				
ID3/AC20	-0.1622	0.1064	-1.52	0.130
ID2/SB	0.02855	0.08982	0.32	0.751
ID3/SB	0.02920	0.08420	0.35	0.729
ID3/AC20/MF+	-0.10334	0.09444	-1.09	0.276
ID3/AC20/MF++	-0.1262	0.1063	-1.19	0.238
NY76	0.02377	0.0418	0.28	0.778
NY96	0.04303	0.0251	0.52	0.603
NY109	-0.2043	0.1114	-1.83	0.070
NY126	-0.00143	0.08715	-0.02	0.987

Table 21(b). Summary of Regression Analysis for Determination of *c*- and ϕ-Values for Abbreviated Protocol (r^2, Adj. = 97.7 %).

Predictor	Coef.	St. Dev.	T	P
Intercept (ID2/AC20)	721.2	114.8	6.28	0.000
Slope (ID2/AC20)	0.55262	0.06187	8.93	0.000
Indicator variables for difference in intercept				
ID2/AC20	-183.5	118.0	-1.56	0.123
ID3/AC20	-130.8	118.3	-1.11	0.272
ID2/SB	-94.4	117.2	-0.81	0.422
ID3/SB	-22.2	118.2	-0.19	0.852
ID3/AC20/MF+	-139.5	118.4	-1.18	0.241
ID3/AC20/MF++	-361.6	143.6	-2.52	0.013
NY76	-465.7	117.5	-3.96	0.000
NY96	-369.5	120.5	-3.07	0.003
NY109	-397.4	119.9	-3.31	0.001
NY126	-336.9	120.2	-2.80	0.006
Indicator variables for difference in slope				
ID2/AC20	0.04439	0.06779	0.65	0.514
ID3/AC20	-0.03541	0.06889	-0.51	0.608
ID2/SB	0.08281	0.06497	1.27	0.205
ID3/SB	0.00493	0.06639	0.07	0.941
ID3/AC20/MF+	-0.04442	0.07022	-0.63	0.528
ID3/AC20/MF++	0.01665	0.07490	0.22	0.825
NY76	0.15167	0.07519	2.02	0.046
NY96	0.10197	0.07905	1.29	0.200
NY109	0.16481	0.07460	2.21	0.029
NY126	0.12987	0.07398	1.76	0.082

Table 21(c). Analysis of Variance for the Regression Analysis.

Source	DF	SS	MS	F	P
Regression	39	23925097	613464	443.11	0.000
Residual Error	105	145369	1384	---	---
Total	144	240070465	---	---	---

Table 22. *C*- and ϕ-Values from Standard Triaxial Tests and Abbreviated Protocol Data.

Mixture	Intercept (kPa)	Slope	C (kPa)	ϕ (degrees)	P (MPa)
From Standard Triaxial Testing					
ID2/AC20	721	0.553	865	33.5	14.4
ID3/AC20	859	0.390	933	23.0	9.2
ID2/SB	735	0.581	903	35.5	16.8
ID3/SB	707	0.582	869	35.6	16.2
ID3/AC20/MF+	802	0.449	898	26.7	10.6
ID3/AC20/MF++	806	0.426	891	25.2	9.8
NY76	374	0.576	457	35.2	8.3
NY96	476	0.596	592	36.6	11.6
NY109	652	0.348	695	20.4	6.1
NY126	503	0.551	603	33.4	10.0
From Abbreviated Protocol					
ID2/AC20	538	0.597	670	36.7	13.2
ID3/AC20	590	0.517	690	31.1	10.1
ID2/SB	627	0.635	812	39.5	18.9
ID3/SB	699	0.558	842	33.9	14.3
ID3/AC20/MF+	582	0.508	675	30.5	9.6
ID3/AC20/MF++	360	0.569	437	34.7	7.8
NY76	256	0.704	360	44.8	11.7
NY96	352	0.655	465	40.9	11.8
NY109	324	0.717	465	45.8	16.2
NY126	384	0.682	526	43.0	15.2

Because it was not clear to the research team which set of parameter estimates were more accurate, and also because neither set was as precise as desired, it was decided to develop a third set of parameter estimates using all available data. The results of this regression analysis are given in Table 23 (parameter estimates) and Table 24 (analysis of variance). The actual intercepts, slopes, *c*- and ϕ-values, and bearing strength p are given in Table 25.

It is clear from the results given in Table 23 that inclusion of all data in the regression analysis has significantly improved the precision of the parameter estimates. The standard deviation for the cohesion estimates (intercepts) using this method ranges from approximately 40 to 50 kPa, whereas the standard deviation values using the standard triaxial data ranged from approximately 130 to 180 kPa. Standard deviations for cohesion estimates using the abbreviated protocol data were all approximately 120 kPa. A similar significant improvement in precision is apparent in the internal friction (slope) estimates, which is probably due to an increase in the

number of data points and an increase in the overall range of the data. The research team, therefore, considers the estimates using the complete data set to be the most reliable.

Table 23. Summary of Regression Analysis for Determination of *c*- and ϕ- Values Using All Available Data (r^2, Adj. = 98.6 %).

Predictor	Coef.	St. Dev.	T	P
Intercept (ID2/AC20)	502.63	28.12	17.88	0.000
Slope (ID2/AC20)	0.66060	0.01895	34.86	0.000
Indicator variables for difference in intercept				
ID3/AC20	64.94	41.31	1.57	0.118
ID2/SB	127.56	38.97	3.27	0.001
ID3/SB	172.89	41.36	4.18	0.000
ID3/AC20/MF+	29.98	40.54	0.74	0.461
ID3/AC20/MF++	-102.55	41.77	-2.46	0.015
NY76	-225.74	38.45	-5.87	0.000
NY96	-148.87	45.43	-3.28	0.001
NY109	-125.18	49.14	-2.55	0.012
NY126	-82.06	47.92	-1.71	0.089
Indicator variables for difference in slope				
ID3/AC20	-0.09986	0.03028	-3.30	0.001
ID2/SB	-0.02767	0.02515	-1.10	0.273
ID3/SB	-0.06876	0.02674	-2.57	0.011
ID3/AC20/MF+	-0.06127	0.02907	-2.11	0.037
ID3/AC20/MF++	0.00636	0.03045	0.21	0.835
NY76	0.00093	0.03399	0.03	0.978
NY96	0.01482	0.03405	0.44	0.664
NY109	-0.06271	0.04227	-1.48	0.140
NY126	-0.04355	0.03686	-1.18	0.240

Table 24. Analysis of Variance for the Regression Analysis.

Source	DF	SS	MS	F	P
Regression	19	23798980	1252578	576.72	0.000
Residual Error	125	271486	2172	---	---
Total	144	24070465	---	---	---

Table 25. *C*- and ϕ-Values Using All Available Data.

Mixture	Intercept (kPa)	Slope	C (kPa)	ϕ (degrees)	P (MPa)
ID2/AC20	510	0.640	664	39.8	15.7
ID3/AC20	568	0.561	685	34.1	11.8
ID2/SB	630	0.633	814	39.3	18.7
ID3/SB	676	0.592	838	36.3	16.2
ID3/AC20/MF+	533	0.599	665	36.8	13.3
ID3/AC20/MF++	400	0.667	537	41.8	14.4
NY76	277	0.662	369	41.4	9.7
NY96	354	0.675	480	42.5	13.4
NY109	377	0.598	471	36.7	9.3
NY126	421	0.617	534	38.1	11.5

To examine the nature of the data gathered and to verify that the relationship between *p*- and *q*-values are reasonable, figures 9 through 18 are presented. These figures are plots of p versus q for each of the ten mixtures included in this study. The data points have been coded so that their source—unconfined compression, confined compression, gyratory compression, or IDT—can be identified. Also included in these figures are the regression equation and the R^2-value. It is clear from these figures that the relationship between *p* and *q* is very strong, is similar for all data types, and, in general, is reasonable.

5.4. Comparison of Triaxial Strength Data and Abbreviated Protocol Data

From examining tables 21(a), 21(b), and 22, several general observations can be made concerning the data generated using the two methods. The standard errors for the regression parameters are almost always somewhat less for the abbreviated protocol than for the standard method. There are probably three reasons for the improved precision of the abbreviated protocol: (1) the specimens are larger; (2) the procedures are simpler; and (3) the range in the data (*p*-values) is greater. Figures 19 through 21 are presented so that the parameter estimates for the mixtures and test methods can be visually compared. There are several other general trends:

- The cohesion values determined using the abbreviated protocol tend to be lower than those found using the standard protocol but in general rank the mixtures similarly.
- The internal friction angles found using the abbreviated protocol tend to be greater than those found using the standard procedure, especially for the N_{design} = 109 mixture.

- The bearing strengths found using the abbreviated protocol tend to be greater than those found using the standard procedure, again, especially for the N_{design} = 109 mixture.
- Parameters estimated using the abbreviated protocol in general agree more closely with those found using the complete data set than do the parameters estimated using the standard triaxial data. This is especially true for the cohesion estimates.

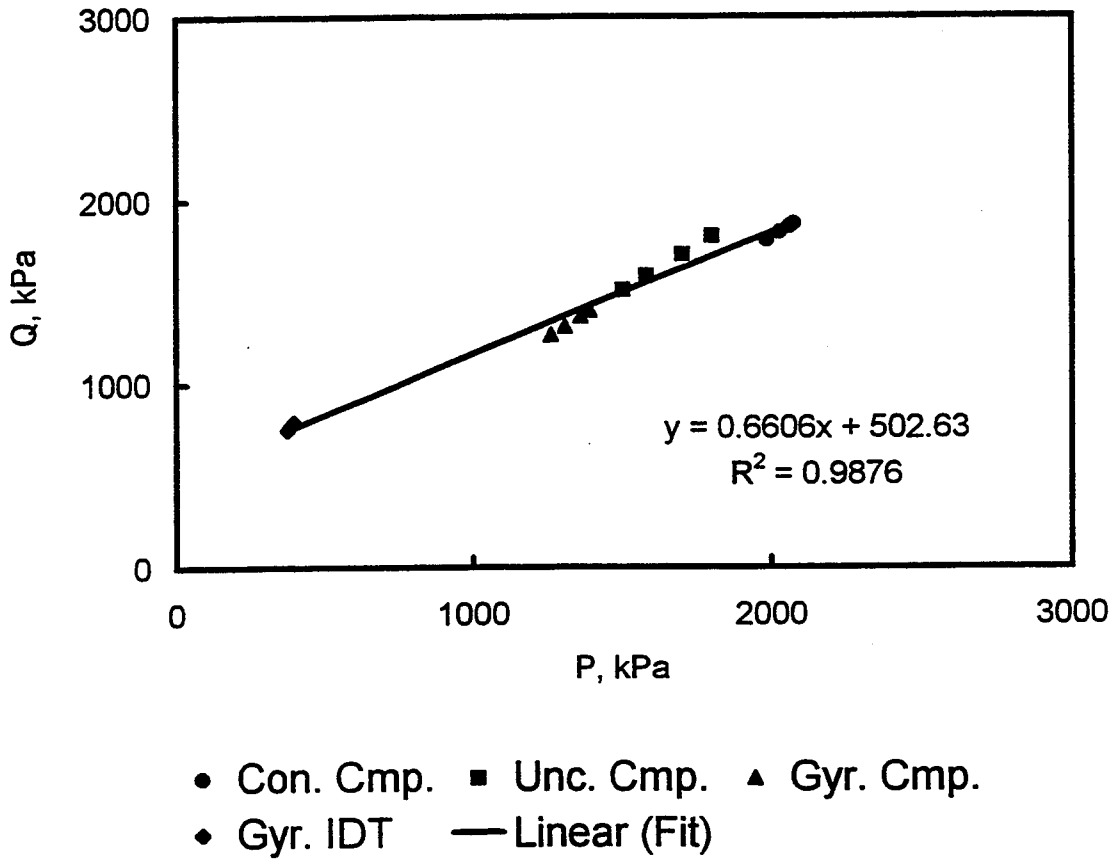

Figure 9. *P*-Q Plot for Mixture ID-2/AC-20 from S.R. 11 Project.

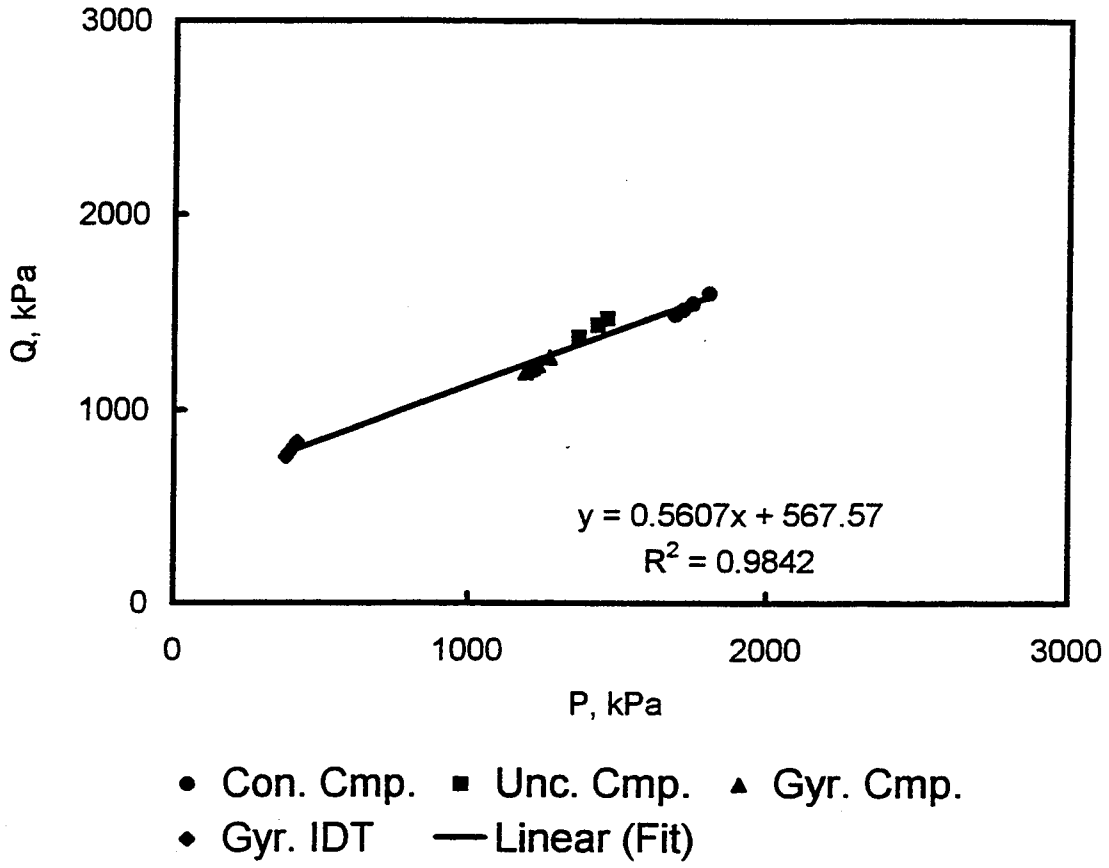

Figure 10. *P*-Q Plot for Mixture ID-3/AC-20 from S.R. 11 Project.

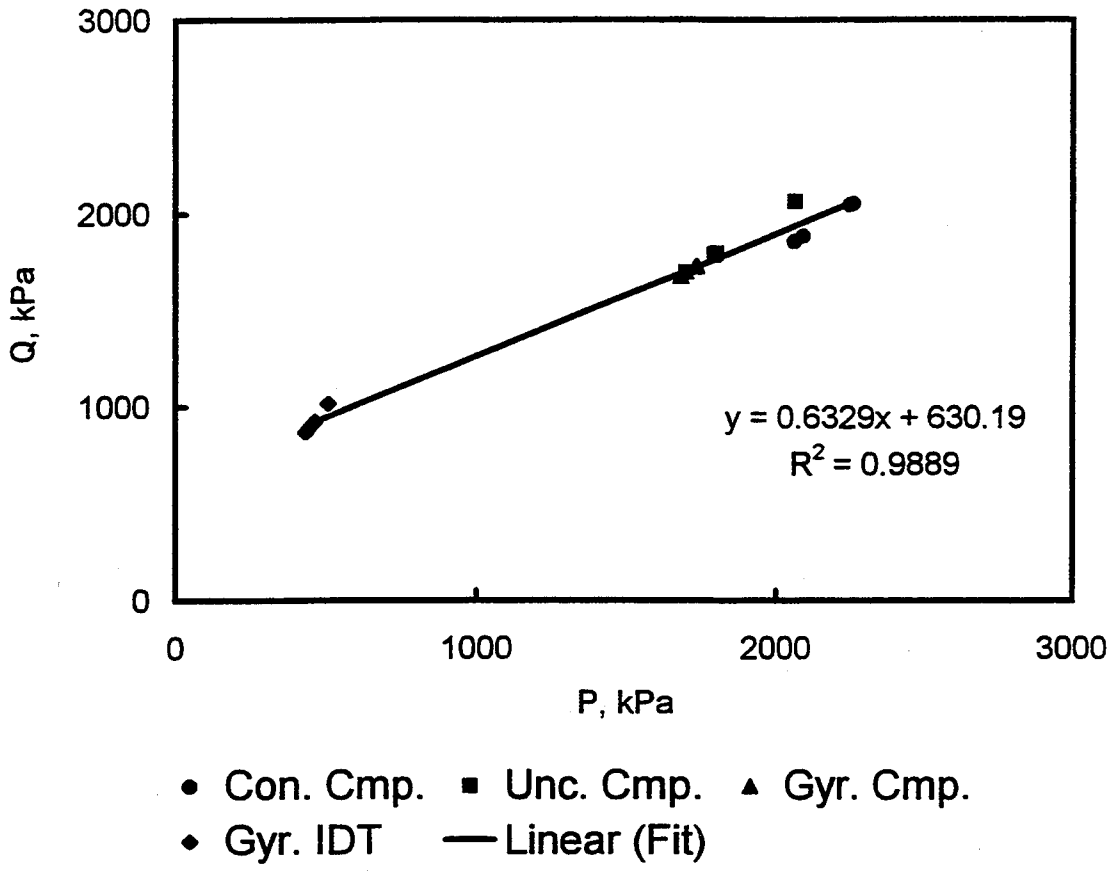

Figure 11. *P*-Q Plot for Mixture ID-2/SB from S.R. 11 Project.

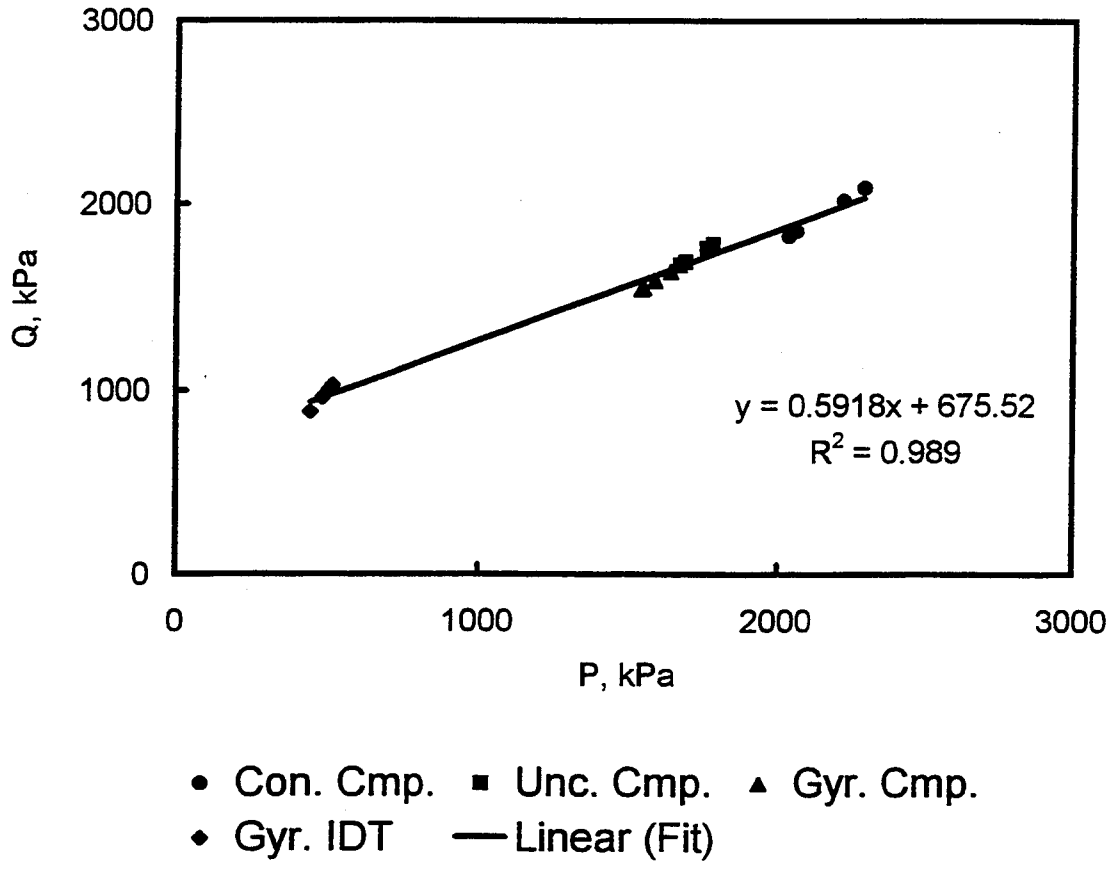

Figure 12. *P*-Q Plot for Mixture ID-3/SB from S.R. 11 Project.

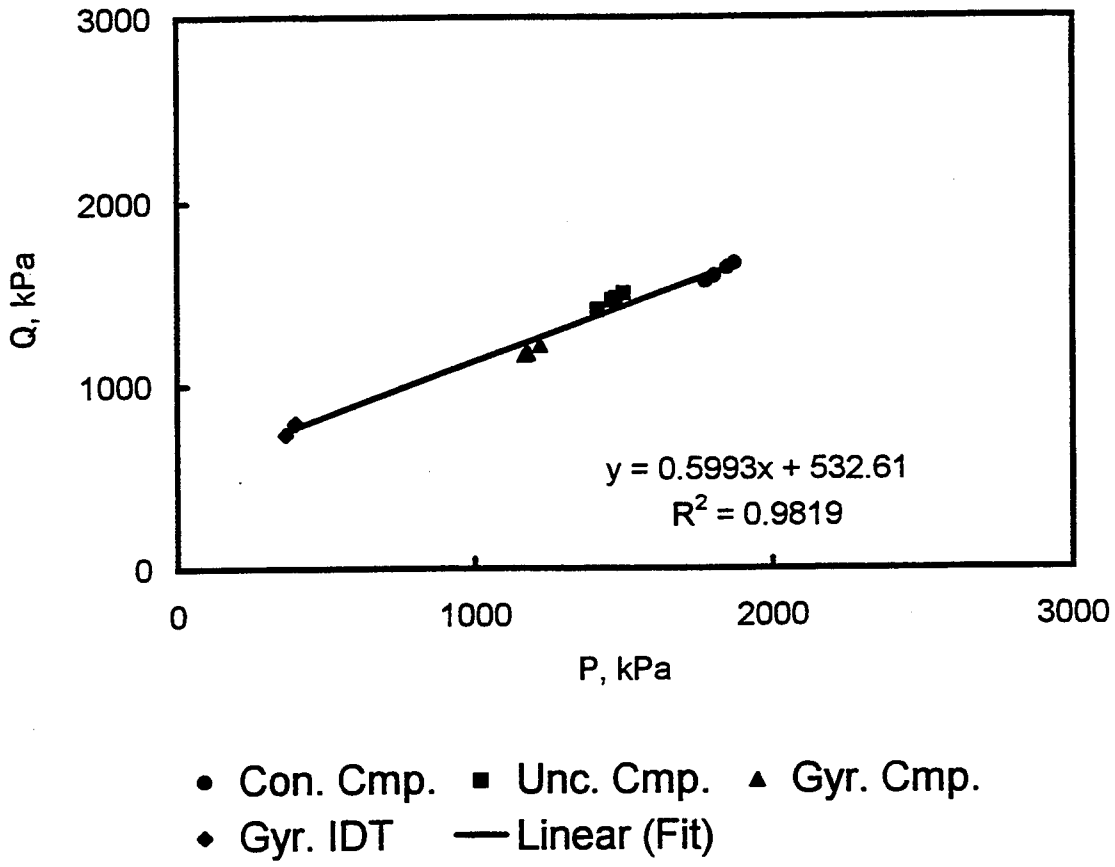

Figure 13. *P*-Q Plot for Mixture ID-3/AC-20/MF+ from S.R. 11 Project.

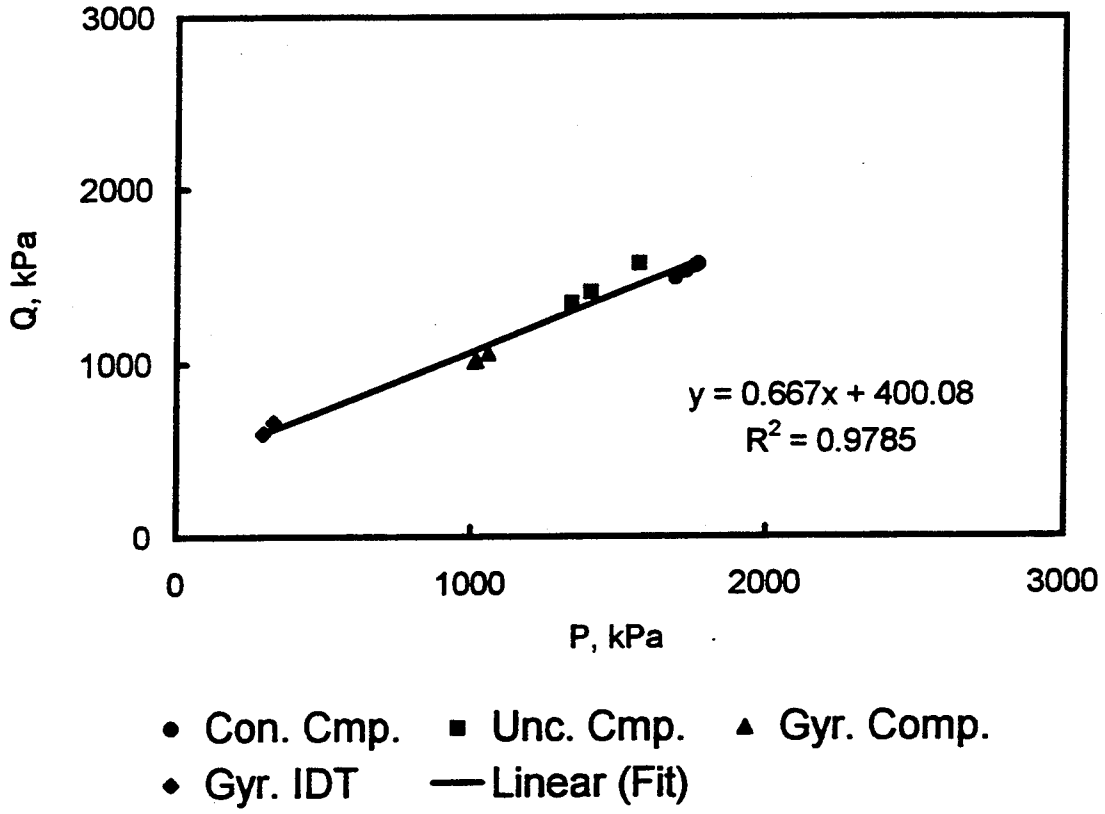

Figure 14. *P*-Q Plot for Mixture ID-3/AC-20/MF++ from S.R. 11 Project.

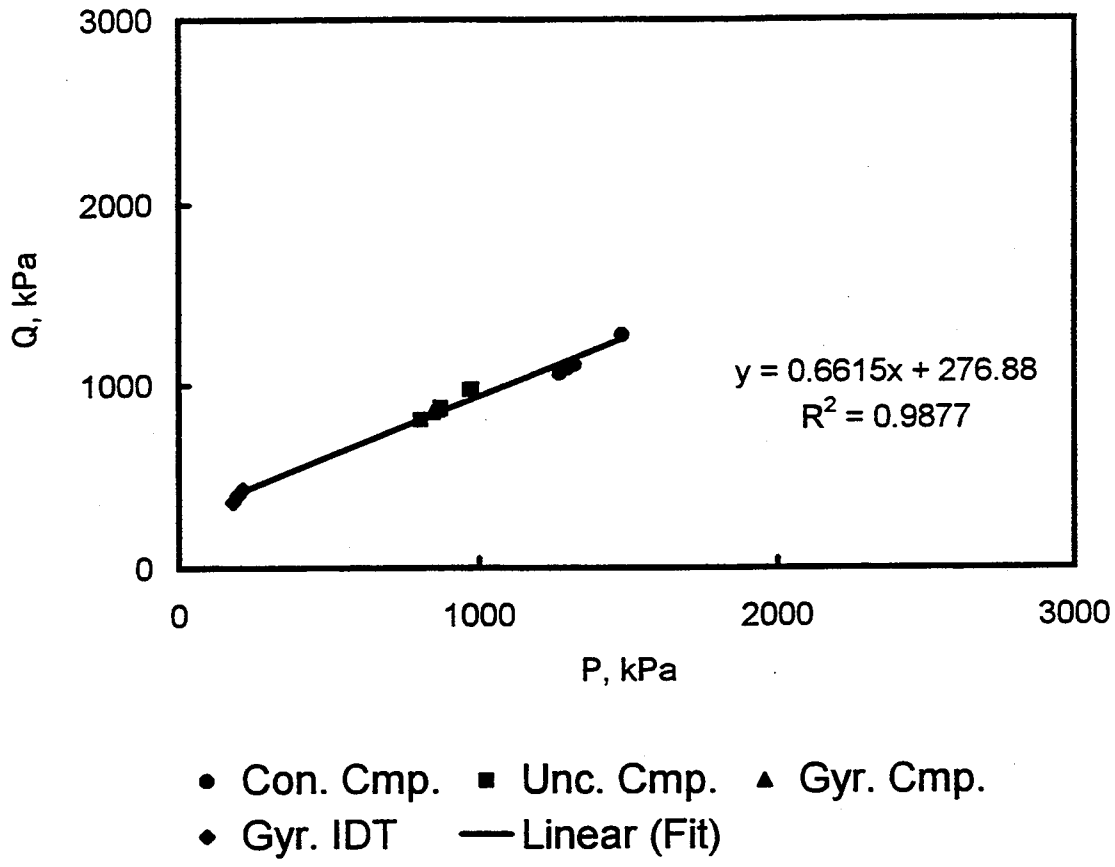

Figure 15. *P*-Q Plot for Mixture NY76 from NY N_{design} Project.

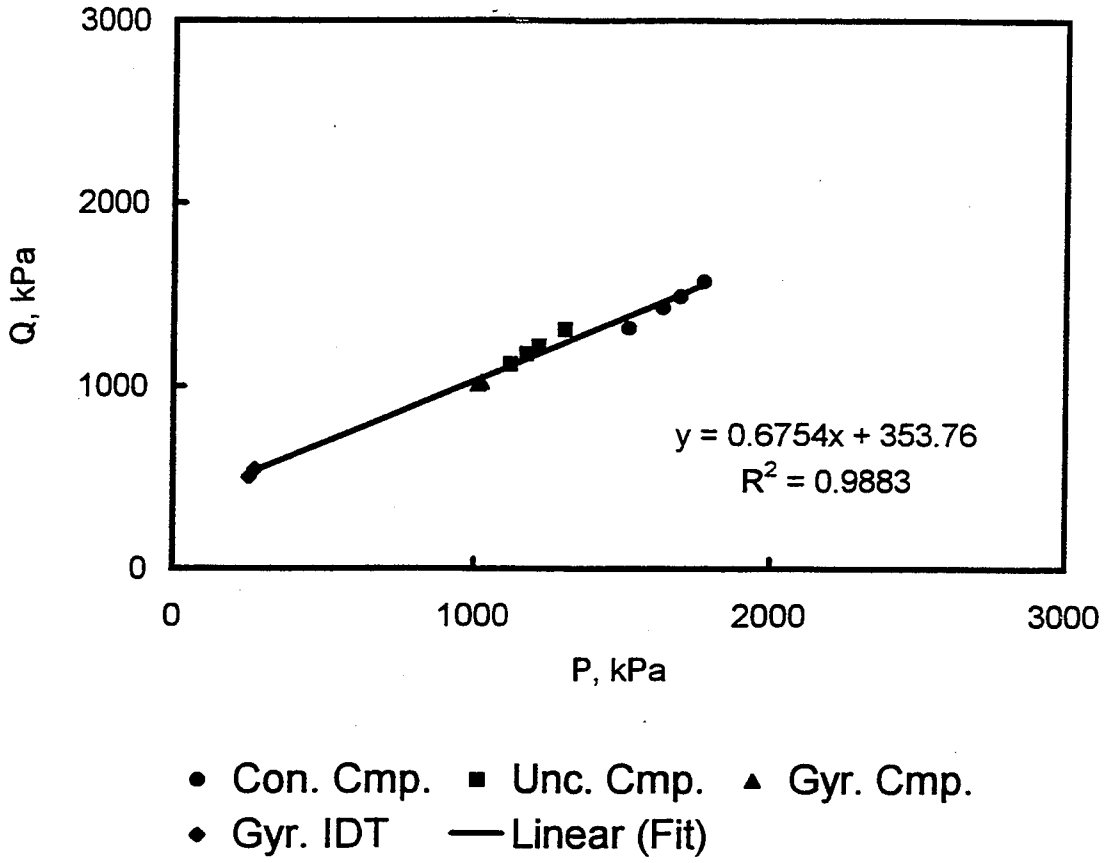

Figure 16. *P*-Q Plot for Mixture NY96 from NY N_{design} Project.

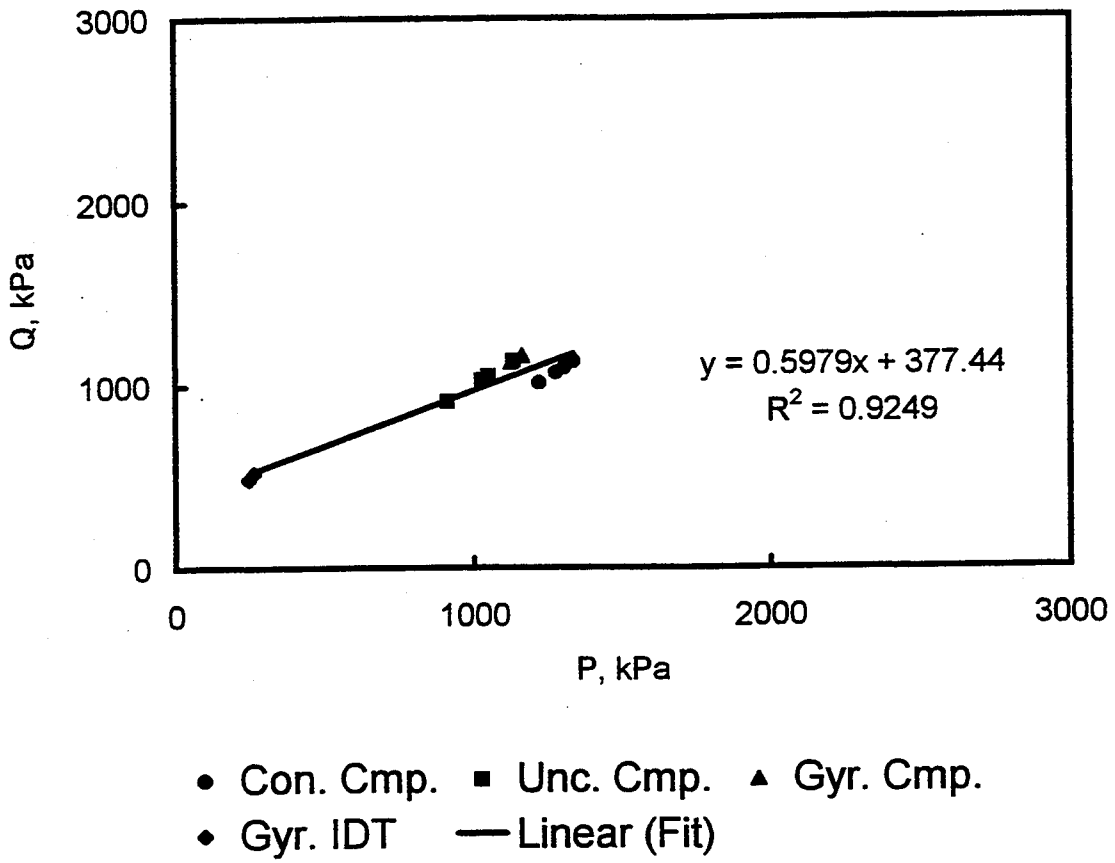

Figure 17. *P*-Q Plot for Mixture NY109 from NY N_{design} Project.

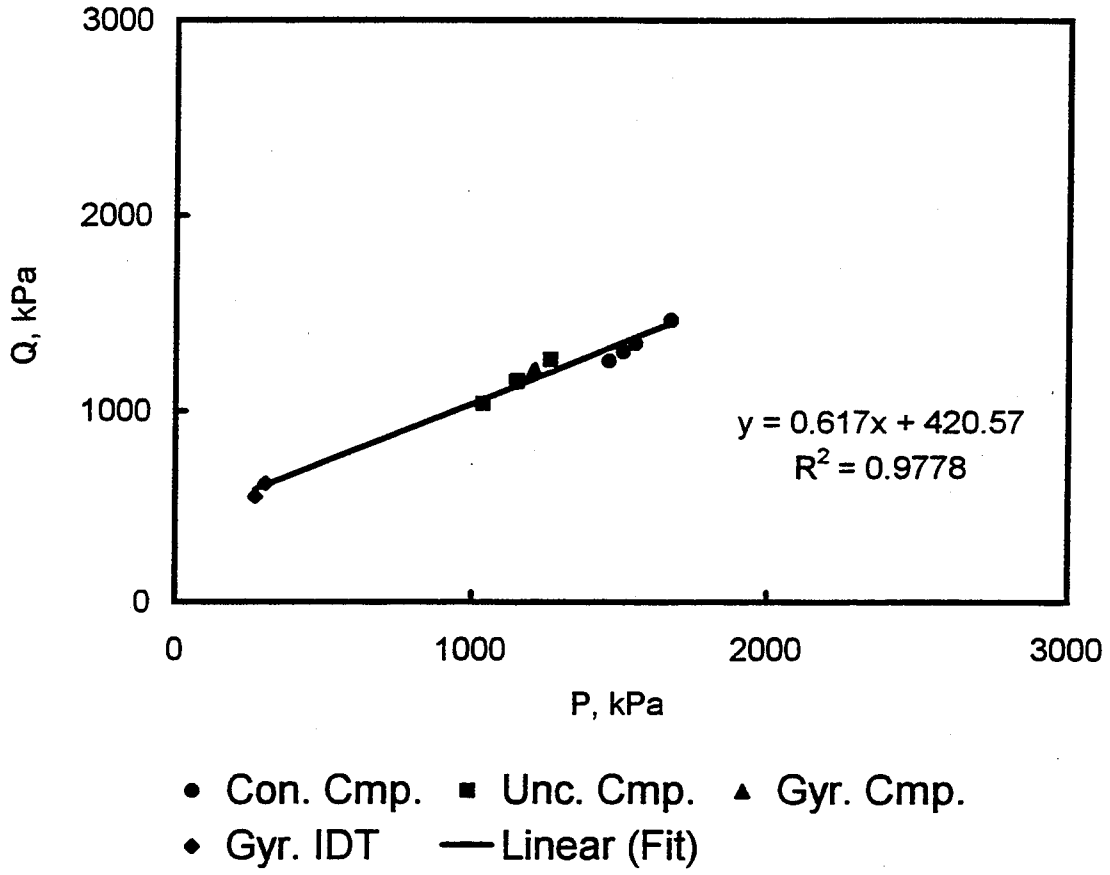

Figure 18. *P*-Q Plot for Mixture NY126 from NY N_{design} Project.

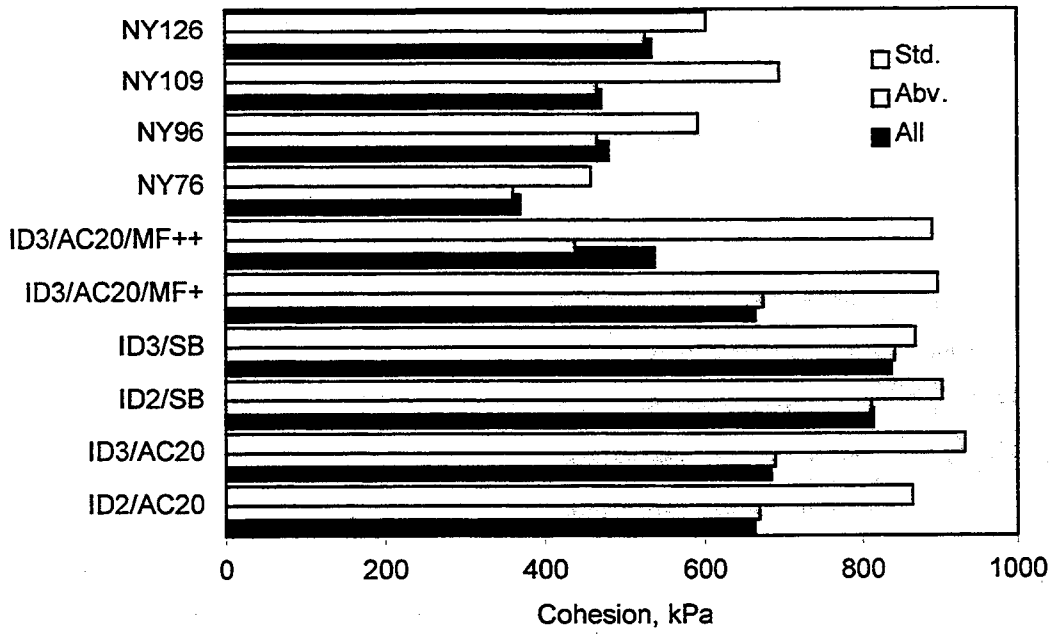

Figure 19. Comparison of CohesionValues as Determined Using Standard Triaxial Tests, Abbreviated Protocol Data, and All Data.

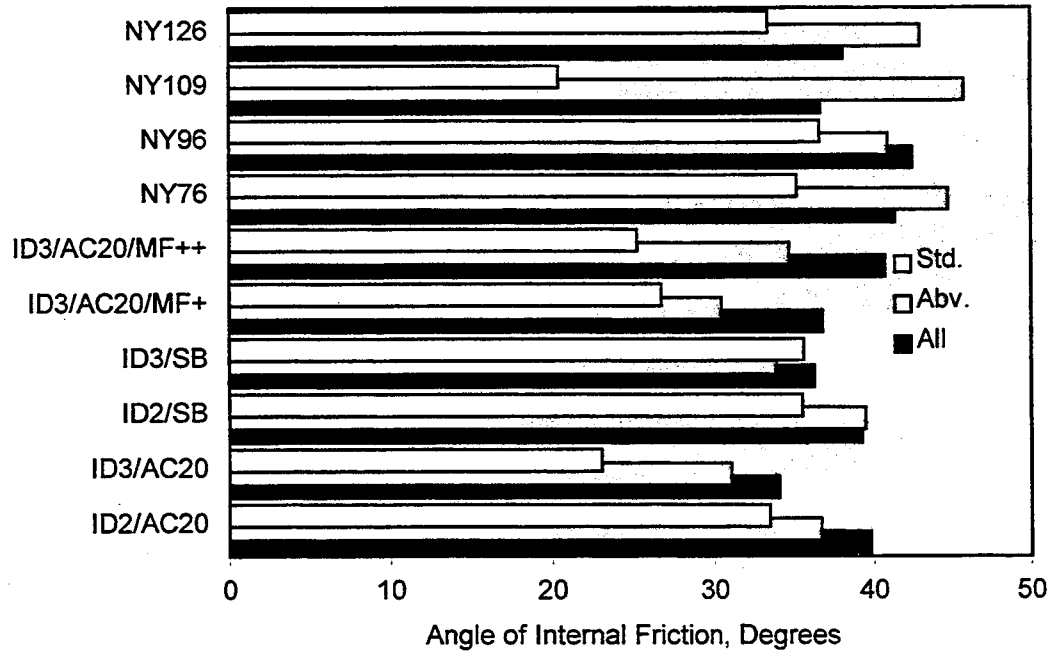

Figure 20. Comparison of Angle of Internal Friction Values as Determined Using Standard Triaxial Tests, Abbreviated Protocol Data, and All Data.

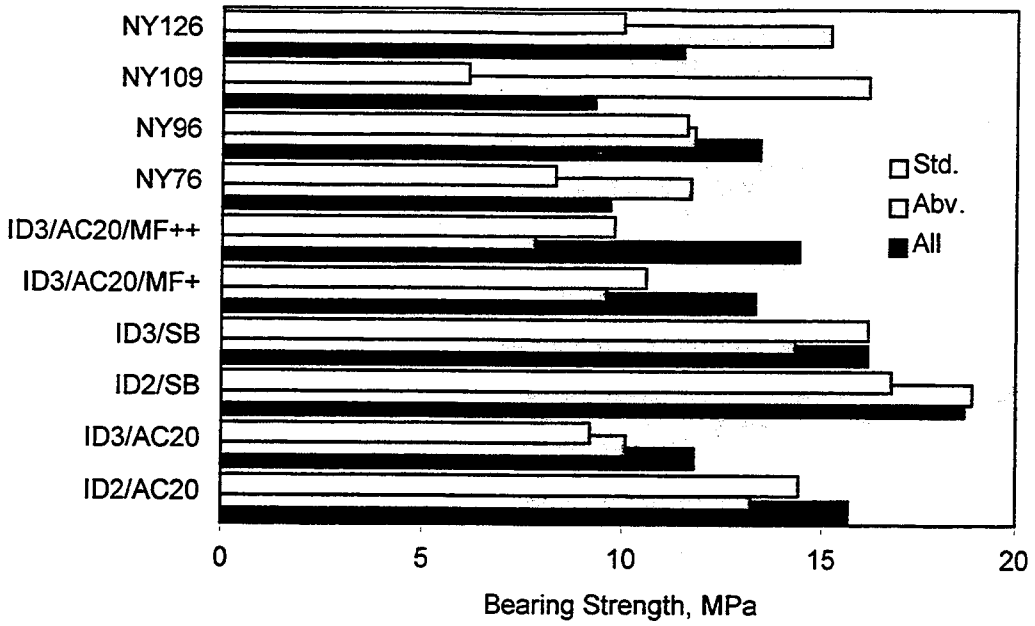

Figure 21. Comparison of Bearing Strength as Determined Using Standard Triaxial Tests, Abbreviated Protocol Data, and All Data.

Although as discussed previously, the precision estimates for the parameters upon which the cohesion and internal friction values are based are most likely inflated, the research team feels that the agreement between the two approaches is fairly good. Furthermore, the abbreviated protocol produced more precise parameter estimates, even though in many cases significantly fewer replicate measurements were made. The abbreviated protocol data seem to agree better with estimates generated using the complete data set, especially when the cohesion is considered. The parameters found using the abbreviated protocol also seem to make better sense intuitively; the SB-modified binder, for example, shows improved cohesion values for the abbreviated protocol but not for the standard method. The bearing strengths found using the abbreviated protocol for the New York mixtures are much more reasonable and consistent with the design traffic levels than those found using the standard procedure. The 109-gyration mixture used on I-81, for example, showed a bearing strength of only 6.1 MPa using standard triaxial data, which was the lowest of any mixture and would indicate that premature rutting would occur under the traffic level found on this highway. The value of 16.2 MPa found using the abbreviated protocol data is consistent with a relatively rut-resistant mixture. This particular mixture was somewhat

difficult to test using the abbreviated protocol because the load did not reach a clear maximum. This might be part of the cause for the unusual data for this mixture.

The research team concludes that the abbreviated protocol is viable and produces relatively accurate estimates of cohesion and internal friction, perhaps even more reliable than those found using standard triaxial data. In general, cohesion values will be lower and internal friction values higher using the abbreviated protocol compared to those found using standard methods. The best possible estimates of the Mohr-Coulomb failure parameters probably could be found by using a combination of IDT tests and compression tests (using either cores or gyratory specimen) under a high level of confinement, perhaps 400 to 600 kPa rather than the 209 kPa used in this study.

An important comparison between the two approaches is the comparison of compressive strength as determined using the 70- by 140-mm cores and as determined using the 150-by-150-mm gyratory specimens. Figure 22 is a plot of compressive strength values determined using the two methods. In most cases, the compressive strength using the gyratory specimens was lower than that using the core. This is unexpected since short aspect ratio specimens normally produce higher compressive strengths because of the effective confinement from end effects. The relatively low compressive strengths could have been the result of using rubber that was too soft, producing greater lateral deformation in the cap than occurring in the specimens. It is also possible that the difference was caused by varying radial distribution of air voids resulting in different average air voids in the gyratory specimens compared to the cores. Further testing should be done to evaluate if 50-durometer rubber inserts might produce better results than the 40-durometer inserts used in this study.

An analysis of variance was performed to statistically compare the compressive strength determined from 70-by-140-mm cores and from the 150-by-150-mm gyratory specimens used for the abbreviated protocol. The results are summarized in Table 26. The analysis of variance confirms that the observed differences in compressive strength with specimen type are statistically significant. Furthermore, as would be expected from Figure 10, the effect of specimen type is mixture specific, as indicated by the high level of significance for the interaction term. Although promising, the results of the analysis of variance indicate that additional refinement in the compressive strength test method for gyratory specimens is needed. As suggested above, a harder rubber insert could improve the results.

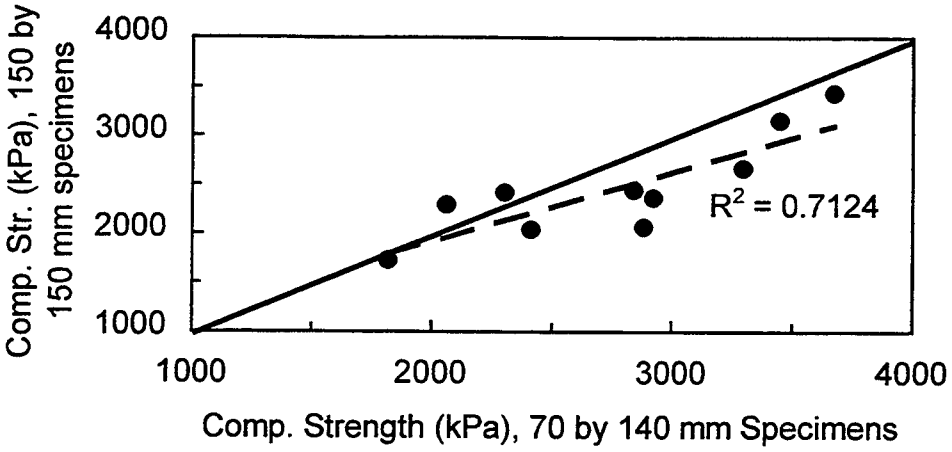

Figure 22. Comparison of Compressive Strength Data Determined Using Standard and Abbreviated Test Procedures.

Table 26. Analysis of Variance for Effect of Specimen Type on Compressive Strength.

Source	DF	Seq SS	Adj SS	Adj MS	F	P
Mix Type	8	19015506	18560819	2320102	105.91	0.000
Specimen Type	1	1248909	948475	948475	43.30	0.000
Mix × Specimen	8	1060976	1060976	132622	6.05	0.000
Error	47	1029598	21906	167	---	---
Total	64	22354989	---	---	---	---

5.5.Effect of N_{design} on *c*- and ϕ- Values

As discussed previously, one of the secondary objectives of this research was to determine if experimentally determined values for mixture cohesion and internal friction would be sensitive to changes in the design compaction level, or N_{design}. The four mixtures from the New York Superpave study used four different levels of compaction, with N_{design} values of 76, 96, 109, and 126. The reader should keep in mind that these were not simply a single aggregate gradation in which the binder content was varied to obtain the proper void content under different levels of compaction. In this case, the aggregates used in the four mixtures were for the most part from different sources. The 76- and 96-gyration mixtures used similar gradations and the same PG 58-28 binder. The 109- and 126-gyration mixtures also used similar gradations (though significantly different from the lower-gyration mixtures) and the same PG 64-28 binder. The four mixtures were, however, carefully designed to have similar binder contents and volumetric properties, despite the differences in N_{design} and constituent materials. Thus the changes in

N_{design}, rather than simply affecting binder content and void content, are in this case associated with more profound and less easily identified mixture properties associated with different compaction effort.

In examining mixture cohesion, as reported in Table 22, increased compaction is clearly associated with increased mixture cohesion, as *c* increases from 369 to 480 kPa for the 76- and 96-gyration mixtures, and from 471 to 534 kPa for the 109- and 126-gyration mixtures. The ϕ-values, on the other hand, increase from 41.4 to 42.5 degrees for the 76- and 96-gyration mixtures and from 36.7 to 38.1 degrees for the 109- and 126-gyration mixtures. Within each set of two mixtures, internal friction increases slightly with increased compaction, though the ϕ-values are significantly lower for the 109- and 126-gyratio mixtures, despite the increased compactive effort. This result initially appears somewhat anomalous, but the reader should keep in mind that a stiffer binder was used in these latter mixtures. Therefore, even though the internal friction of the mixture was less, additional compactive effort was required for the 109- and 126-gyration mixtures because of the stiffer binder. The simultaneous changes in various compositional characteristics for these four mixtures make interpretation of the results somewhat difficult. However, it does seem clear that as expected, changes in N_{design} are reflected in the measured cohesion and internal friction for the four New York mixtures.

5.6. Comparison of Strength Data and c and ϕ Values with Field Performance of S.R.11 Mixtures.

As discussed previously, field data on rutting exists only for the S.R. 11 mixtures. Estimated rut depths at a traffic level of 1 million ESALs was estimated for each of the four primary S.R. 11 mixtures included in this study and were presented in Table 3. Because of this limited data, elaborate analyses of strength parameters and observed rut resistance cannot be performed. The approach used here involved calculation of R^2 values for simple linear relationships between observed rutting and primary strength parameters:

- cohesion, *c*
- angle of internal friction, ϕ
- bearing strength, *p*
- unconfined compressive strength
- confined compressive strength
- indirect tension strength

Also included in this analysis was the maximum permanent shear strain (MPSS) from the repeated shear at constant height data. The RSCH test has become recognized as perhaps the most reliable laboratory test for characterizing rut resistance and has been included here to further evaluate relationships between triaxial data and permanent deformation. For the Mohr-Coulomb failure parameters c and ϕ, and for bearing strength and unconfined compressive strength, R^2-values were determined using data from the standard triaxial data, the abbreviated protocol data, and the combined data set (unconfined compressive strength for the combined data is the average of the two methods). Confined strength was available only for standard triaxial data, and indirect tensile strength was available only for abbreviated protocol data. The R^2-values for these relationships are summarized in Table 27.

Table 27. R^2-Values for Field Rutting and Triaxial Strength Parameters.

Method	R^2-Value for Parameter						
	RSCH MPSS (%)	C (kPa)	ϕ (deg)	P (MPa)	Comp. Str. (kPa)	Con. Str. (kPa)	IDT Str. (kPa)
SST	81	---	---	---	---	---	---
Standard Triaxial	---	0	20	31	35	31	---
Abbreviated Protocol	---	93	4	38	68	---	96
Combined Data	---	95	1	27	54	---	---

Note that strong relationships are apparent for only four cases: RSCH data, cohesion from the abbreviated protocol and combined data sets, and IDT strength values. These latter two correlations may appear to be potentially spurious because traditional pavement engineering practice has emphasized the importance of internal friction in developing good rut resistance; however, as will be seen in the section below, the data in this study strongly suggest that cohesion plays a more important role in the rut resistance of mixtures than has previously been believed. To further examine the relationship between cohesion and field rutting, Figure 23 is presented, in which estimated rut depth at 1 million ESALs is plotted as a function of cohesion, as determined using the abbreviated protocol.

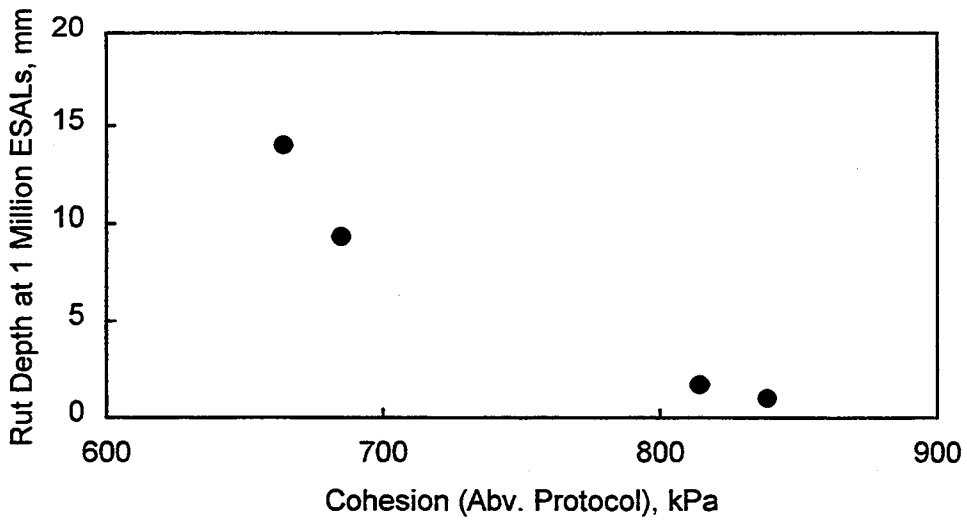

Figure 23. Plot of Rut Depth at 1 Million ESALs As a Function of Cohesion for S.R. 11 Mixtures.

5.7.Comparison of Strength Data and *c*- and ϕ- Values with Repeated Shear at Constant Height Data

An approach similar to that in evaluating relationships between triaxial strength parameters and field performance data has been used to evaluate relationships between triaxial strength parameters and repeated shear at constant height test results. This portion of the research was meant to further evaluate the utility of *c*, ϕ, and related parameters in characterizing the rut resistance of asphalt concrete mixtures. Currently, the RSCH test is the most widely used test for evaluating the resistance of asphalt concrete mixtures to permanent deformation.

Simple, linear regression analyses were performed between triaxial strength parameters and maximum permanent shear strain as determined in the RSCH test. These analyses were done, where possible, with three sets of data: standard triaxial data, abbreviated data, and the full data set. The results are summarized in Table 28. The overall best predictor of MPSS is the mixture cohesion, with R^2-values of 76, 62, and 74 % for the standard, abbreviated, and full data set, respectively. The unconfined compressive strength (standard protocol) and IDT strength were the single best predictors of MPSS, with R^2-values of 81 % and 80 %, respectively, which are extremely high values for these types of relationships in asphalt concrete mixtures. Another good predictor was confined compressive strength (R^2 = 76 %). Although internal friction determined using the abbreviated protocol was also a good predictor of RSCH test results, with R^2=77 %, examination of a plot of these parameters shows that maximum permanent shear strain

increases with increasing angle of internal friction, which is counter-intuitive. The research team believes that increased internal friction is not in fact reducing the performance of the mixture, but instead, as internal friction increases, it tends to reduce mixture cohesion, which causes a reduction in rut resistance. Furthermore, R2-values for mixture cohesion and unconfined and confined compressive strength (standard protocol) and IDT strength are very high—86 %, 84 % and 99 %, respectively—indicating that it is in fact mixture cohesion rather than internal friction which controls strength, and thus rut resistance, for typical dense-graded asphalt concrete mixtures.

These strong relationships between RSCH data and mixture cohesion, and especially IDT strength, may at first seem confusing and potentially spurious; however, the RSCH is performed without confinement and was specifically developed in this way because the SHRP A-003A research team believed that this represented the critical condition for rutting in flexible pavements (Monismith et. al., 1994). In other words, the RSCH is essentially a measure of unconfined shear strength under *repeated* loading. Mixture cohesion, c, as defined in this report, represents the unconfined shear strength under *monotonic* loading; therefore, it should not be surprising that mixture cohesion as measured in triaxial testing relates to the MPSS determined using the repeated shear test. This simply indicates that the strength of asphalt concrete mixtures under repeated loading is strongly related to the strength under monotonic loading.

The good relationship between the IDT and the RSCH test is easily explainable in that the IDT test is a very good estimate of mixture cohesion. An illustration of this relationship is given in Figure 24, in which mixture cohesion, as determined from the combined data set, is plotted as a function of IDT strength. The relationship is very strong; assuming the intercept is zero, the mixture cohesion can be estimated as $c = 1.75\ \sigma_{IDT}$, with an R^2-value of 98 %.

This relationship is not at all surprising. As shown graphically in Figure 25, the stress state in the IDT test is such that the average normal stress, $p = (\sigma_{Y\text{-}IDT} + \sigma_{X\text{-}IDT})/2$, is close to 0. Therefore, at this point, the value of the maximum shear stress, $q = (\sigma_{Y\text{-}IDT} - \sigma_{X\text{-}IDT})/2$, will be slightly greater than the mixture cohesion, c, assuming a Poisson's ratio of 0.5, $p = -\sigma_{X\text{-}IDT}$ and $q = -2\sigma_{X\text{-}IDT}$. Because the average normal stress for the IDT stress state is so close to zero, the differences in angle of internal friction among typical asphalt concrete mixtures has little effect on the relationship between cohesion and maximum shear stress during the IDT test; thus, cohesion can be accurately estimated from the IDT strength as $c \approx 1.75\sigma_{IDT}$.

Table 28. R^2-Values for Triaxial Strength Parameters and Maximum Permanent Shear Strain from the RSCH Test.

Method	R^2-Value for Parameter					
	C (kPa)	ϕ (deg)	P (MPa)	Comp. Str. (kPa)	Con. Str. (kPa)	IDT Str. (kPa)
Standard Triaxial	76	0	39	81	76	---
Abbreviated Protocol	62	77	3	41	---	80
Combined Data	74	12	46	67	---	---

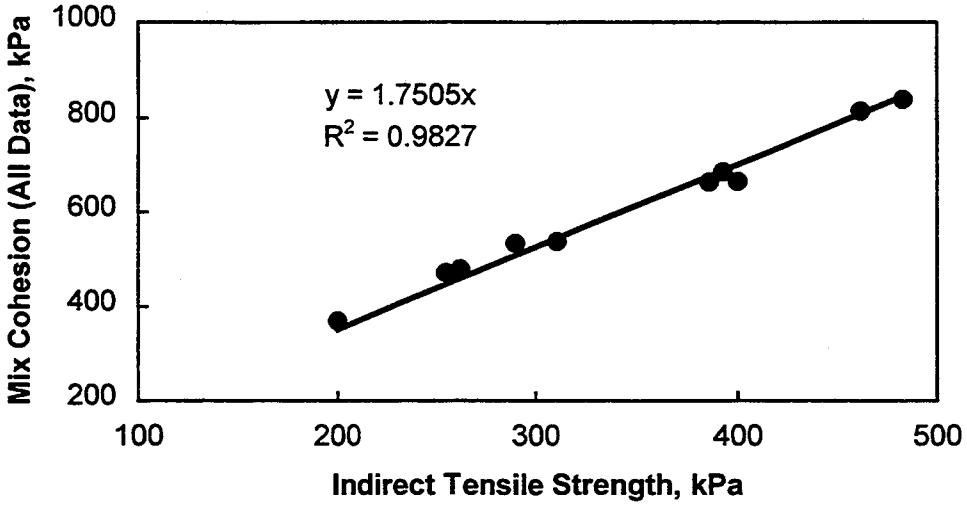

Figure 24. Relationship Between Mixture Cohesion and IDT Strength.

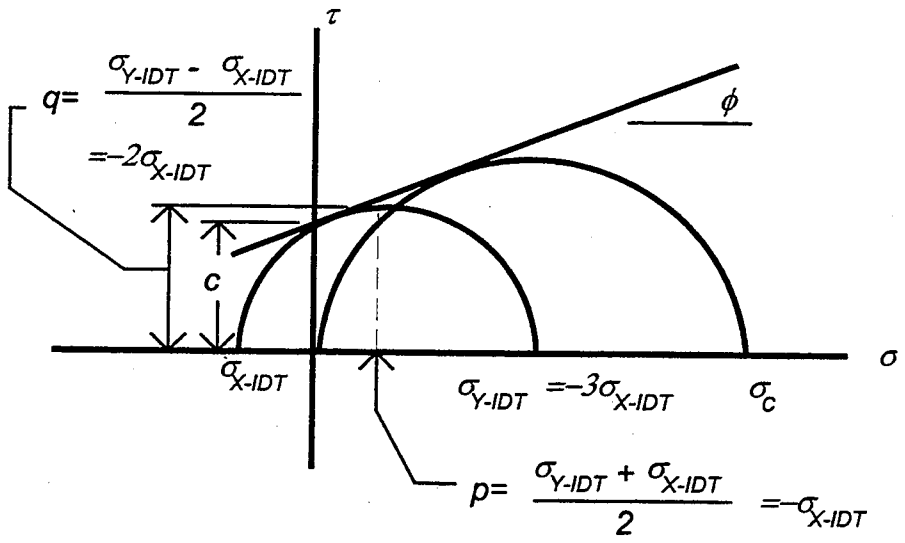

Figure 25. Construction of Mohr's Circle for IDT Test and Related Mohr-Coulomb Failure Parameters.

6. DISCUSSION

The results and analysis presented previously strongly indicate that the triaxial strength test is a useful means of characterizing the rut resistance of asphalt concrete mixtures. Of great significance is the finding that mixture cohesion is potentially of greater importance in determining rut resistance than internal friction in currently used asphalt concrete wearing course mixtures. A second important finding is that abbreviated protocol appears to provide cohesion and internal friction estimates as good as or even better than those found using the conventional approach. The IDT strength, in particular, provides an excellent indication of mixture cohesion, which in turn is strongly related to mixture rut resistance. The IDT strength test would appear to be an extremely promising test for mixture design and especially quality control/quality assurance (QC/QA) testing since the IDT test can be easily performed on very thin field cores. In the laboratory, the IDT test can be combined with a simple unconfined compression to provide additional information on internal friction, which could be useful in forensic studies and in evaluating unusual mixtures.

It is important to note that the good relationships observed between triaxial strength parameters and field rutting and repeated shear test data would not have existed had not the triaxial strength testing conditions been carefully devised to be approximately rheologically equivalent to traffic loading (and RSCH test conditions). Many studies of the triaxial test and other static test methods have been unsuccessful in the past because of using slow testing rates at relatively high temperatures. Under these conditions, the importance of binder to the response becomes minimal, and the test becomes simply a means of evaluating aggregate internal friction under unrealistic loading conditions. Thus, another important finding of this study is that the principle of rheological equivalence must be applied in comparing asphalt concrete mixture data gathered under different loading rates.

To further demonstrate the utility of the triaxial strength tests, a final series of analyses was done in an attempt to correlate Mohr-Coulomb failure parameters with mixture properties which should relate to cohesion and internal friction. Since these mixtures contained similar good quality cubical aggregates with similar values for air voids, VMA, and VFA, the research team felt that the main parameters which should influence mixture cohesion and internal friction would be binder consistency at high temperature and aggregate gradation, respectively. To

evaluate the first hypothesis—that mixture cohesion should be related to binder grade—linear regression analyses were run using binder high-temperature PG-grade as the predictor variable and mixture cohesion as the dependent variable. The R^2-values found were 37 %, 75 %, and 77 % using the standard, abbreviated, and full data sets, respectively. This strongly supports the use of the IDT strength test in triaxial testing to gain better estimates of mixture cohesion, and also shows that the expected relationship between binder grade and cohesion does, in fact, exist. Figure 26 is a plot of mixture cohesion versus PG-grade; clearly, as binder high-temperature grade increases, mixture cohesion increases. The scatter in the plot is due to other factors affecting cohesion, which should include mineral filler content, binder content, VFA, and aggregate-binder interactions.

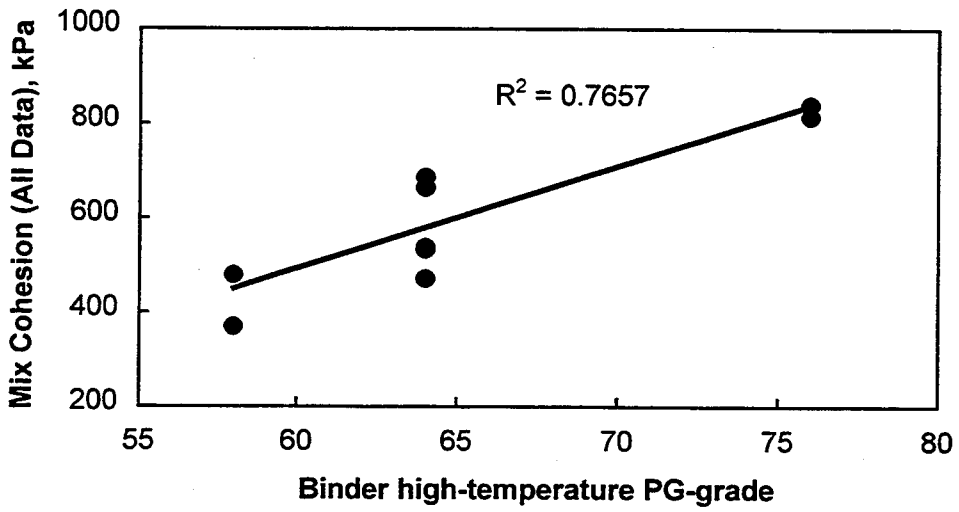

Figure 26. Relationship Between Mixture Cohesion and Binder High-Temperature PG-Grade.

The second hypothesis—that aggregate gradation should strongly influence internal friction—was evaluated in the following way. The research team believed that the more a gradation deviates from the maximum density gradation, the greater the internal friction will be for mixtures containing that aggregate. The deviation from the maximum density gradation was quantified as follows. The actual percent passing for each aggregate was subtracted from the calculated maximum density gradation, squared, and averaged for each sieve in the gradation (from 0.075 mm to the first sieve passing 100 %). In other words, the deviation from maximum

density was characterized using the root-mean-squared (RMS) method. When linear regression was used to compare this parameter with the angle of internal friction ϕ for the various mixtures, R^2-values of 10 %, 90 %, and 45 % were found using the standard, abbreviated, and full data set, respectively. The abbreviated protocol ϕ-values were the only ones showing a strong relationship with aggregate gradation, which was exceptional. Figure 27 is a plot angle of internal friction versus RMS deviation from maximum density. Clearly, as deviation from maximum density increases, angle of internal friction also increases. Furthermore, this strongly suggests that not only does the abbreviated protocol approach yield better estimates of mixture cohesion, but it also provides more meaningful estimates of internal friction.

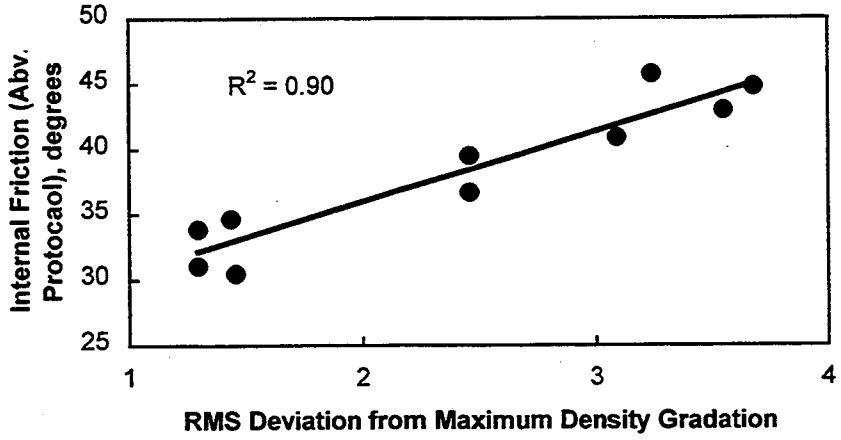

Figure 27. Relationship Between Mixture Internal Friction and Aggregate Deviation (RMS) from Maximum Density Gradation.

Some additional discussion is needed concerning the apparent lack of influence of internal friction on rut resistance. The research team believes that this lack of influence is in part due to the relatively high levels of internal friction found in current asphalt concrete mixtures. Particularly since the widespread use of Superpave, most aggregates used in asphalt concrete are good quality, cubical, abrasion-resistant aggregates that deviate significantly from the maximum density gradation. Under these conditions, internal friction should be so good that for currently used mixtures, poor internal friction is not a cause for poor resistance to permanent deformation. If asphalt concrete mixtures containing poor-quality, rounded aggregates following a maximum

density gradation were to be evaluated, then the research team believes that internal friction would show greater significance in contributing to mixture rut resistance.

A second important factor in determining the relative importance of cohesion and internal friction in developing rut resistance is the recent finding that truck tires, especially the now widely used radial designs, produce significant tensile stresses at the pavement surface (Engle and Roque, 1999). The combination of high tire pressures and surface tensile stresses could result in a critical combination of relatively high shear stresses and low levels of confinement—just the sort of stress state existing in both the RSCH and IDT tests. In other words, the presence of large surface tensile stresses under truck tires should be expected to reduce the degree of confinement in the pavement so that the critical stress state for rutting involves little or no confinement.

The research team believed at the onset of the study that the concept of bearing strength as a rational basis for designing mixtures to resist permanent deformation was very promising; however, the concept of bearing capacity as currently conceived is apparently not effective in predicting rut resistance. This is most likely due to the relatively large tensile and shear stresses occurring on the surface of a pavement under traffic loading. In practice, the best simple test for evaluating rut resistance of Superpave mixtures appears to be the indirect tension test, run at 3.75 mm/min at a temperature 20 °C below the critical pavement temperature for permanent deformation. Mixtures made with aggregates meeting Superpave requirements are unlikely to fail from lack of internal friction. Based upon Asphalt Institute guidelines for interpreting maximum permanent shear strains from the RSCH test (Bukowski and Harman, 1997) and the relationship observed in this study between MPSS and IDT strength, guidelines can be generated for evaluating rut resistance on the basis of IDT strength tests. In Figure 28, MPSS is plotted as a function of IDT strength; the relationship, as expected, is very strong with $R^2 = 92$ %. Using this relationship and the Asphalt Institute guidelines, preliminary guidelines for interpreting IDT strength tests have been developed and are given in Table 29. These guidelines must only be applied for the test conditions used in this study—a test temperature 20 °C below the 7-day average maximum pavement temperature and a loading rate of 3.75 mm/min.

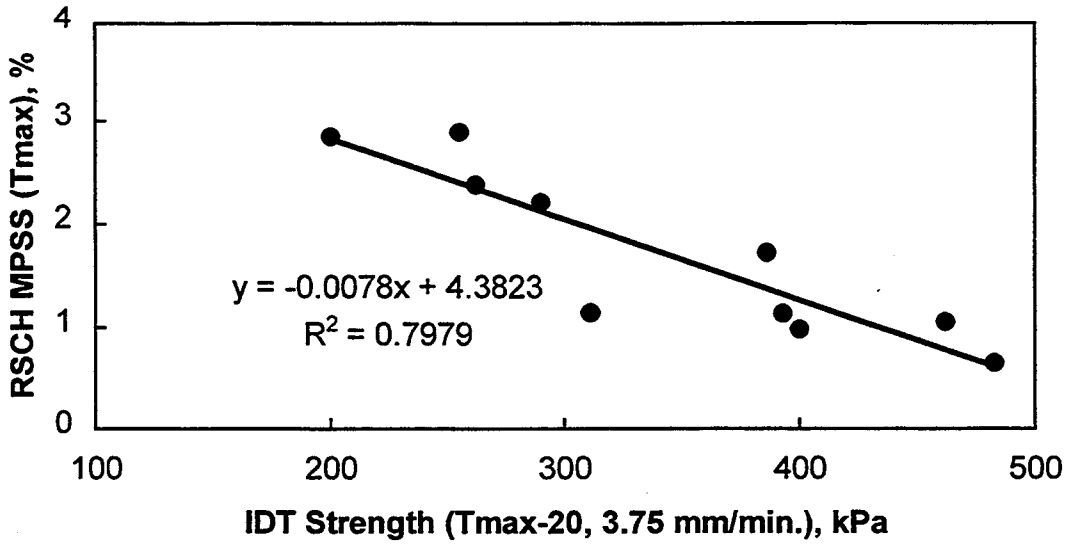

Figure 28. Relationship Between RSCH Maximum Permanent Shear Strain and IDT Strength.

Table 29. Guidelines for Evaluating Rut Resistance Using IDT Strength.

RSCH Max. Perm Shear Strain %	IDT Strength kPa	Rut Resistance
< 1.0	> 440	Excellent
1.0 to < 2.0	> 320 to 440	Good
2.0 to < 3.0	> 200 to 320	Fair
≥ 3.0	200 ≥	Poor

Even though in most cases, current mix designs following Superpave (or similar) guidelines for aggregate angularity and gradation are unlikely to fail because of poor internal friction, in some cases it might be necessary to evaluate internal friction. Measurements of internal friction would be advisable when investigating failures or in evaluating unusual aggregates, binders, or mixture additives. In such cases, unconfined compressive strength tests can be combined with IDT tests to calculate angle of internal friction. Based upon the results of this study, guidelines for evaluating mixture internal friction are given in Table 30. Again, these guidelines are only applicable when the test conditions used in this study are followed—test temperature 20 °C below the 7-day average maximum pavement temperature and a loading rate of 7.5 mm/min for compression tests and 3.75 mm/min for IDT strength tests.

When using the guidelines in tables 29 and 30, the pavement technologist should keep in mind that mixture cohesion, as indicated by IDT strength, will normally be more important than internal friction in determining rut resistance. Based upon the results of this study, most Superpave mixtures should exhibit internal friction angles of about 40 ° and higher (using the abbreviated protocol), which should be adequate for ensuring rut resistance, provided mixture cohesion is adequate.

Table 30. Guidelines for Evaluating Angle of Internal Friction (abbreviated protocol).

Angle of Internal Friction, ϕ Degrees	**Rating**
> 45	Excellent
> 40 to 45	Good
> 35 to 40	Fair
35 ≥	Poor

The research team feels that the results of this study are positive enough to warrant provisional implementation without further study; however, further research should be performed to extend and refine the conclusions and recommendations. Specific recommendations for further research are given in the following section. Of particular significance in implementation is the current use of AASHTO T-283 as an integral part of the Superpave mixture design and analysis system. This procedure already involves IDT testing of gyratory specimens, although the temperature is somewhat lower and the loading rate somewhat higher than that used in this project; however, this might provide useful data for verifying and extending the results of this study. Furthermore, a relatively minor modification in AASHTO T-283, such as an increase in test temperature, could make this test useful and an indication of both rut resistance and moisture resistance without any additional investment or effort by contractors, hot-mix plants, highway departments, or testing laboratories. However, additional research is needed to adapt and refine the IDT test for use in designing and analyzing asphalt concrete mixtures. Of special importance is developing a simple and repeatable procedure for performing IDT strength tests at higher temperatures.

7. CONCLUSIONS AND RECOMMENDATIONS

A total of 10 asphalt concrete wearing course mixtures were tested in this study. These mixtures used good-quality, angular aggregates, with gradations that, in general, deviated somewhat from the maximum density gradation. Most of the mixtures exhibited aggregate, binder, and volumetric properties consistent with current Superpave guidelines. The strength tests performed in this study were done at a temperature 20 °C lower than the 7-day average maximum pavement temperature at a rate of 7.5 mm/min for compression tests and 3.75 mm/min for IDT tests. The abbreviated protocol used gyratory specimens 150 mm in diameter and 100 mm high for IDT testing and 150 mm high for compression testing. These compression tests were performed employing reusable end caps for portland cement concrete testing with 40-durmoeter neoprene inserts. Standard triaxial tests were performed on 70-mm-diameter-by-140-mm-high cores taken from gyratory specimens tested in a standard triaxial pressure cell with no confinement and under 209 kPa confinement. Based upon the testing and analysis conducted during this research project, the research team has made the following conclusions and recommendations:

1. The abbreviated protocol for determining triaxial strength parameters provided more precise and meaningful estimates of mixture cohesion and internal friction than the standard method.
2. Unconfined compressive strength tests on 150-by-150-mm gyratory specimens, employing reusable end caps with neoprene inserts, provided results comparable to those found testing 70-mm-diameter-by-140-mm-high cores.
3. The concept of rheological equivalence, in which time-temperature superposition is approximately applied to provide equivalent loading under static laboratory tests to that which occurs during traffic loading, or during rapid laboratory tests.
4. For the types of asphalt concrete wearing course mixtures currently being used, made using good quality aggregates deviating significantly from maximum density gradations, mixture cohesion appears to relate more closely to rut resistance than internal friction.
5. The IDT strength test can be used to accurately estimate mixture cohesion, using the relationship $c \approx -1.75\sigma_{IDT}$.

6. Good correlations were observed between RSCH maximum permanent shear strain and mixture cohesion. IDT strength correlated extremely well with maximum permanent shear strain.
7. For currently used asphalt concrete mixtures, mixture cohesion appears to relate strongly to binder high-temperature PG grade. Mixture internal friction appears to relate most strongly to deviation of the aggregate gradation from the maximum density gradation.
8. The IDT strength test can be used as an extremely simple and accurate performance-related test for evaluating the resistance to permanent deformation of asphalt concrete mixtures. It is especially attractive for QC/QA testing because of the simplicity and low cost of the test and the potentially good repeatability. Furthermore, very thin field cores could easily be tested using this method.
9. The IDT strength test should be implemented on a provisional basis in order to gather further information on the relationship between IDT strength and rut resistance. This could be easily done using a modified protocol involving testing at the standard IDT loading rate of 50 mm/min. but a higher temperature than that used in this project.
10. The following issues should be addressed in further research addressing the use of triaxial strength and related tests in evaluating mixture rut resistance:
    - Can AASHTO T-283 data be gathered for a wide range of projects, along with field performance and RSCH data where available, to provide a quick means of verifying and extending the results of this research?
    - What is the relationship between IDT strength data gathered using AASHTO T-283 and that gathered using the test procedures suggested in this study?
    - Is the internal friction, as measured using the abbreviated protocol, sensitive to poor quality aggregates, such as poorly crushed gravel and natural sand?
    - Is the angle of internal friction sensitive to aggregate gradations passing through the restricted zone?
    - Can mixture cohesion as measured using the IDT test be used to estimate optimum binder content for Superpave mixtures?
    - What are the relationships among mixture volumetric parameters, binder grade, and mixture cohesion?
    - Will the strong relationships seen in this study exist for a wider range of mixtures and environmental conditions?
    - Can the loading rates and temperatures used in this study be increased to better simulate traffic loading conditions?

- Should the 40-durometer rubber used in the specimen end caps in the compressive strength tests on gyratory specimens be replaced with harder 50-durometer rubber?
- Can a modified bearing strength theory be developed using both tire pressures and surface stresses that can then be used as a rational basis for mixture design to resist permanent deformation?
- How should the indirect tensile strength test be modified to maximize repeatability at higher temperatures?

8. REFERENCES

American Association of State Highway and Transportation Officials. *AASHTO Provisional Standards*. Washington, D.C.: American Association of State Highway and Transportation Officials, June 1996, 614 pp.

American Association of State Highway and Transportation Officials. *Standard Specifications for Transportation Materials and Methods of Sampling and Testing*. Washington, D.C.: American Association of State Highway and Transportation Officials, 1999.

American Society for Testing and Materials. *Annual Book of ASTM Standards*. Conshohocken, PA: American Society for Testing and Materials, 1999, 996 pp.

Anderson, D. A., D. W. Christensen, R. Dongre, M. G. Sharma, J. Runt, and P. Jourdahl. *Asphalt Behavior at Low Service Temperatures*, Final Report to the Federal Highway Administration. PTI Report No. 8802. University Park, PA: The Pennsylvania Transportation Institute, January 1989, 318 pp.

Anderson, M.R., G. A. Huber, R.B. McGennis, R.Bonaquist, R. W. May, and T. W. Kennedy. *Evaluation and Update of Design Gyrations for the Superpave Gyratory Compactor (N_{desig}II Experiment)*, Draft Final Report, April 8, 1999.

Asphalt Institute, *Superpave Mix Design (SP-2)*, Lexington, KY: The Asphalt Institute, 1996, 117 pp.

Barksdale, R. G. "Compressive Stress Pulse Times in Flexible Pavements for Use in Dynamic Testing." *Highway Research Record 345*, 1971, Highway Research Board, pp. 32-44.

Bowles, J. E. *Physical and Geotechnical Properties of Soils*. New York: McGraw-Hill Book Co., 1979, 478 pp.

Bukowski, J. R., and T. Harman. *Minutes of the Superpave Mixture Report Task Group*, Meeting of September 1997.

Christensen, D. W., and T. Handojo. "Comparison of the Mechanical Properties of Asphalt Concrete at Determined from Shear and Indirect Tension Tests." Submitted for consideration for presentation and publication to the Association of Asphalt Paving Technologists, July 1999.

Fee, Frank. *Relationship of SHRP Binder Tests to Field Performance*. Pennsauken, NJ: Koch Materials Co., September 1993.

Hewitt, W. H. "Analysis of Various Flexible Paving Mixtures by a Theoretical Design Procedure Based on Shear Strength." Paper prepared for presentation at the Annual Meeting of the Highway Research Board, July 1964.

Huang, Y. *Pavement Analysis and Design.* Prentice Hall Publishing Co., 1993.

Huschek, S., "The Deformation Behavior of Asphaltic Concrete Under Triaxial Compression." *Proceedings of the Association of Asphalt Paving Technologists*, Vol. 54, 1985, pp. 407-426.

Kalcheff, I. V., and R. G. Hicks. "A Test Program for Determining the Resilient Properties of Granular Materials." *Journal of Testing and Evaluation*, Vol.1, No. 6, American Society for Testing and Materials, pp. 472-479.

Krutz, Neil C. and Peter E. Sebaaly. "The Effects of Aggregate Gradation on Permanent Deformation of Asphalt Concrete." *The Journal of the Association of Asphalt Paving Technologists*, Vol. 62, 1993, pp. 450-473.

Monismith, C. L., *Permanent Deformation Response of Asphalt Aggregate Mixes, Report SHRP A-415*, National Research Council, Washington D.C., 1994.

Myers, L. A., R. Roque, and B. E. Ruth. "Mechanisms of Surface-Initiated Longitudinal Wheel Path Cracks in High-Type Bituminous Pavements." *Journal of the Association of Asphalt Paving Technologists*, Vol. 67, 1998, pp. 401-428.

Neter, J., W. Wasserman, and M. H. Kutner. *Applied Linear Statistical Models.* Homewood, IL: Irwin, 1985, 1127 pp.

Nijboer, L. W., *Plasticity as a Factor in the Design of Dense Bituminous Road Carpets.* New York: Elsevier Publishing Co., Inc., 1948, 184 pp.

Pennsylvania Department of Transportation (PennDOT), *Commonwealth of Pennsylvania Department of Transportation Publication 408*, 1994.

Ramirez, T.L. *Research Project 91-58A Anti-Rutting Materials for Intersections, Annual Performance Inspection (Year 4)*, Internal PennDOT Field Report, October, 1995.

Sebaaly, P. E., and N. C. Krutz. "The Effects of Aggregate Gradation on Permanent Deformation of Asphalt Concrete." *Journal of the Association of Asphalt Paving Technologists*, Vol. 62, 1993, pp. 450-477.

University of Maryland Department of Civil Engineering. *Interim Task C Report: Preliminary Recommendations for the Simple Performance Test.* College Park, MD: University of Maryland Department of Civil Engineering, May 15, 1998, 60 pp.

APPENDIX: PROJECT DATA

Project	Agg. Grad.	Binder	N-design	Mix Code	Air Voids	Spec. Size, Dia. by Ht.	Test Type	Con. Stress	p	q	p, Corr. For Voids	q, Corr. For Voids	Dev. Stress	Dev. Str., Corr. For Voids
					%	mm		kPa	kPa	kPa	kPa	kPa	kPa	kPa
SR11	PA-ID2	PG 76-28	N/A	S2	4.1	70 x 140	Unc. Comp.	0	2048	2048	2064	2064	4096	4127
SR11	PA-ID2	PG 76-28	N/A	S2	4.5	70 x 140	Con. Comp.	207	2172	1965	2252	2045	3930	4089
SR11	PA-ID2	PG 76-28	N/A	S2	4.0	70 x 140	Unc. Comp.	0	1696	1696	1696	1696	3392	3392
SR11	PA-ID2	PG 76-28	N/A	S2	4.3	70 x 140	Con. Comp.	207	2213	2006	2261	2054	4013	4108
SR11	PA-ID2	PG 76-28	N/A	S2	4.5	70 x 140	Unc. Comp.	0	1710	1710	1790	1790	3420	3579
SR11	PA-ID2	PG 76-28	N/A	S2	4.5	70 x 140	Con. Comp.	207	2013	1806	2093	1886	3613	3772
SR11	PA-ID2	PG 76-28	N/A	S2	4.1	70 x 140	Unc. Comp.	0	1779	1779	1795	1795	3558	3590
SR11	PA-ID2	PG 76-28	N/A	S2	4.3	70 x 140	Con. Comp.	207	2013	1806	2061	1854	3613	3709
SR11	PA-ID3	PG 76-28	N/A	S3	4.3	70 x 140	Unc. Comp.	0	1620	1620	1668	1668	3241	3336
SR11	PA-ID3	PG 76-28	N/A	S3	3.9	70 x 140	Con. Comp.	207	2075	1869	2059	1853	3737	3705
SR11	PA-ID3	PG 76-28	N/A	S3	3.8	70 x 140	Unc. Comp.	0	1717	1717	1685	1685	3434	3370
SR11	PA-ID3	PG 76-28	N/A	S3	4.3	70 x 140	Con. Comp.	207	1986	1779	2034	1827	3558	3653
SR11	PA-ID3	PG 76-28	N/A	S3	4.4	70 x 140	Unc. Comp.	0	1717	1717	1781	1781	3434	3561
SR11	PA-ID3	PG 76-28	N/A	S3	3.5	70 x 140	Con. Comp.	207	2372	2165	2292	2085	4330	4171
SR11	PA-ID3	PG 76-28	N/A	S3	4.0	70 x 140	Unc. Comp.	0	1758	1758	1758	1758	3516	3516
SR11	PA-ID3	PG 76-28	N/A	S3	3.8	70 x 140	Con. Comp.	207	2255	2048	2223	2016	4096	4032
SR11	PA-ID2	AC20	N/A	A2	3.6	70 x 140	Unc. Comp.	0	1765	1765	1701	1701	3530	3403
SR11	PA-ID2	AC20	N/A	A2	3.8	70 x 140	Con. Comp.	207	2020	1813	1988	1782	3627	3563
SR11	PA-ID2	AC20	N/A	A2	4.4	70 x 140	Unc. Comp.	0	1738	1738	1801	1801	3475	3602
SR11	PA-ID2	AC20	N/A	A2	4.4	70 x 140	Con. Comp.	207	1965	1758	2029	1822	3516	3644
SR11	PA-ID2	AC20	N/A	A2	4.5	70 x 140	Unc. Comp.	0	1503	1503	1583	1583	3006	3165
SR11	PA-ID2	AC20	N/A	A2	4.4	70 x 140	Unc. Comp.	0	1441	1441	1505	1505	2882	3010
SR11	PA-ID2	AC20	N/A	A2	4.6	70 x 140	Con. Comp.	207	1965	1758	2061	1854	3516	3708
SR11	PA-ID2	AC20	N/A	A2	4.4	70 x 140	Con. Comp.	207	2013	1806	2077	1870	3613	3740
SR11	PA-ID3	AC20	N/A	A3	3.5	70 x 140	Unc. Comp.	0	1448	1448	1368	1368	2896	2737
SR11	PA-ID3	AC20	N/A	A3	3.6	70 x 140	Unc. Comp.	0	1496	1496	1433	1433	2992	2865
SR11	PA-ID3	AC20	N/A	A3	3.8	70 x 140	Con. Comp.	207	1834	1627	1802	1595	3254	3191
SR11	PA-ID3	AC20	N/A	A3	3.9	70 x 140	Con. Comp.	207	1765	1558	1749	1542	3117	3085
SR11	PA-ID3	AC20	N/A	A3	3.6	70 x 140	Con. Comp.	207	1779	1572	1715	1508	3144	3017
SR11	PA-ID3	AC20	N/A	A3	3.5	70 x 140	Con. Comp.	207	1772	1565	1692	1486	3130	2971
SR11	PA-ID3	AC20	N/A	A3	3.8	70 x 140	Unc. Comp.	0	1496	1496	1464	1464	2992	2929
SR11	PA-ID3	AC20	N/A	A3MF+	4.2	70 x 140	Unc. Comp.	0	1469	1469	1500	1500	2937	3001

Project	Agg. Grad.	Binder	N-design	Mix Code	Air Voids	Spec. Size, Dia. by Ht.	Test Type	Con. Stress	p	q	p, Corr. For Voids	q, Corr. For Voids	Dev. Stress	Dev. Str., Corr. For Voids
					%	mm		kPa	kPa	kPa	kPa	kPa	kPa	kPa
SR11	PA-ID3	AC20	N/A	A3MF+	3.7	70 x 140	Unc. Comp.	0	1510	1510	1462	1462	3020	2924
SR11	PA-ID3	AC20	N/A	A3MF+	3.8	70 x 140	Con. Comp.	207	1806	1600	1775	1568	3199	3136
SR11	PA-ID3	AC20	N/A	A3MF+	4.2	70 x 140	Con. Comp.	207	1772	1565	1804	1597	3130	3194
SR11	PA-ID3	AC20	N/A	A3MF+	4.0	70 x 140	Con. Comp.	207	1848	1641	1848	1641	3282	3282
SR11	PA-ID3	AC20	N/A	A3MF+	4.0	70 x 140	Unc. Comp.	0	1476	1476	1476	1476	2951	2951
SR11	PA-ID3	AC20	N/A	A3MF+	4.3	70 x 140	Unc. Comp.	0	1365	1365	1413	1413	2730	2826
SR11	PA-ID3	AC20	N/A	A3MF+	4.2	70 x 140	Con. Comp.	207	1841	1634	1873	1666	3268	3332
SR11	PA-ID3	AC20	N/A	A3MF++	3.9	70 x 140	Unc. Comp.	0	1358	1358	1342	1342	2717	2685
SR11	PA-ID3	AC20	N/A	A3MF++	4.2	70 x 140	Con. Comp.	207	1662	1455	1694	1487	2910	2973
SR11	PA-ID3	AC20	N/A	A3MF++	3.7	70 x 140	Unc. Comp.	0	1455	1455	1407	1407	2910	2814
SR11	PA-ID3	AC20	N/A	A3MF++	3.5	70 x 140	Con. Comp.	207	1841	1634	1761	1554	3268	3109
SR11	PA-ID3	AC20	N/A	A3MF++	3.7	70 x 140	Con. Comp.	207	1820	1613	1772	1566	3227	3131
SR11	PA-ID3	AC20	N/A	A3MF++	4.0	70 x 140	Con. Comp.	207	1731	1524	1731	1524	3048	3048
SR11	PA-ID3	AC20	N/A	A3MF++	3.6	70 x 140	Unc. Comp.	0	1634	1634	1570	1570	3268	3141
NY		PG 64-28	109	NY109	4.1	70 x 140	Con. Comp.	207	1207	1000	1223	1016	2000	2031
NY		PG 64-29	109	NY109	4.5	70 x 140	Unc. Comp.	0	1055	1055	1135	1135	2110	2269
NY		PG 64-30	109	NY109	4.4	70 x 140	Unc. Comp.	0	986	986	1050	1050	1972	2099
NY		PG 64-31	109	NY109	4.1	70 x 140	Unc. Comp.	0	1014	1014	1029	1029	2027	2059
NY		PG 64-32	109	NY109	4.1	70 x 140	Con. Comp.	207	1262	1055	1278	1071	2110	2142
NY		PG 64-33	109	NY109	4.3	70 x 140	Con. Comp.	207	1289	1083	1337	1130	2165	2261
NY		PG 64-34	109	NY109	3.8	70 x 140	Unc. Comp.	0	945	945	913	913	1889	1826
NY		PG 64-35	109	NY109	3.8	70 x 140	Con. Comp.	207	1338	1131	1306	1099	2262	2198
NY		PG 64-36	126	NY126	4.2	70 x 140	Unc. Comp.	0	1007	1007	1039	1039	2013	2077
NY		PG 64-37	126	NY126	4.5	70 x 140	Unc. Comp.	0	1076	1076	1155	1155	2151	2311
NY		PG 64-38	126	NY126	4.5	70 x 140	Con. Comp.	207	1386	1179	1466	1259	2358	2517
NY		PG 64-39	126	NY126	4.1	70 x 140	Con. Comp.	207	1496	1289	1512	1305	2579	2611
NY		PG 64-40	126	NY126	4.2	70 x 140	Unc. Comp.	0	1117	1117	1149	1149	2234	2298
NY		PG 64-41	126	NY126	4.2	70 x 140	Unc. Comp.	0	1234	1234	1266	1266	2468	2532
NY		PG 64-42	126	NY126	4.4	70 x 140	Con. Comp.	207	1489	1282	1553	1346	2565	2692
NY		PG 64-43	126	NY126	4.2	70 x 140	Con. Comp.	207	1641	1434	1673	1466	2868	2932
NY		PG 58-28	76	NY76	3.8	70 x 140	Unc. Comp.	0	841	841	809	809	1682	1619
NY		PG 58-29	76	NY76	4.0	70 x 140	Unc. Comp.	0	972	972	972	972	1944	1944

Project	Agg. Grad.	Binder	N-design	Mix Code	Air Voids	Spec. Size, Dia. by Ht.	Test Type	Con. Stress	p	q	p, Corr. For Voids	q, Corr. For Voids	Dev. Stress	Dev. Str., Corr. For Voids
					%	mm		kPa	kPa	kPa	kPa	kPa	kPa	kPa
NY		PG 58-30	76	NY76	4.0	70 x 140	Unc. Comp.	0	876	876	876	876	1751	1751
NY		PG 58-31	76	NY76	4.5	70 x 140	Unc. Comp.	0	896	896	976	976	1793	1952
NY		PG 58-32	76	NY76	4.2	70 x 140	Con. Comp.	207	1289	1083	1321	1114	2165	2229
NY		PG 58-33	76	NY76	3.8	70 x 140	Con. Comp.	207	1303	1096	1271	1064	2193	2129
NY		PG 58-34	76	NY76	4.1	70 x 140	Con. Comp.	207	1282	1076	1298	1092	2151	2183
NY		PG 58-35	76	NY76	4.3	70 x 140	Con. Comp.	207	1434	1227	1482	1275	2455	2550
NY		PG 58-36	96	NY96	4.5	70 x 140	Unc. Comp.	0	1096	1096	1176	1176	2193	2352
NY		PG 58-37	96	NY96	4.2	70 x 140	Unc. Comp.	0	1276	1276	1307	1307	2551	2615
NY		PG 58-38	96	NY96	3.9	70 x 140	Unc. Comp.	0	1234	1234	1218	1218	2468	2437
NY		PG 58-39	96	NY96	3.8	70 x 140	Unc. Comp.	0	1151	1151	1120	1120	2303	2239
NY		PG 58-40	96	NY96	4.1	70 x 140	Con. Comp.	207	1510	1303	1526	1319	2606	2638
NY		PG 58-41	96	NY96	4.2	70 x 140	Con. Comp.	207	1607	1400	1638	1432	2799	2863
NY		PG 58-42	96	NY96	4.3	70 x 140	Con. Comp.	207	1648	1441	1696	1489	2882	2978
NY		PG 58-43	96	NY96	3.6	70 x 140	Con. Comp.	207	1841	1634	1777	1570	3268	3141
SR11	PA-ID2	PG 76-28	N/A	S2	4.4		Unc. Comp.	0	1727	1727	1727	1727	3454	3454
SR11	PA-ID2	PG 76-28	N/A	S2	4.3	150 x 150	Unc. Comp.	0	1729	1729	1729	1729	3458	3458
SR11	PA-ID2	PG 76-28	N/A	S2	4.1	150 x 150	Unc. Comp.	0	1731	1731	1731	1731	3462	3462
SR11	PA-ID2	PG 76-28	N/A	S2	4.3	150 x 150	Unc. Comp.	0	1678	1678	1678	1678	3356	3356
SR11	PA-ID3	PG 76-28	N/A	S3	4.1	150 x 150	Unc. Comp.	0	1635	1635	1635	1635	3270	3270
SR11	PA-ID3	PG 76-28	N/A	S3	4.2	150 x 150	Unc. Comp.	0	1546	1546	1546	1546	3092	3092
SR11	PA-ID3	PG 76-28	N/A	S3	4.1	150 x 150	Unc. Comp.	0	1584	1584	1584	1584	3168	3168
SR11	PA-ID3	PG 76-28	N/A	S3	4.2	150 x 150	Unc. Comp.	0	1540	1540	1540	1540	3080	3080
SR11	PA-ID2	AC-20	N/A	A2	4.3	150 x 150	Unc. Comp.	0	1308	1308	1308	1308	2616	2616
SR11	PA-ID2	AC-20	N/A	A2	4.5	150 x 150	Unc. Comp.	0	1393	1393	1393	1393	2786	2786
SR11	PA-ID2	AC-20	N/A	A2	4.2	150 x 150	Unc. Comp.	0	1262	1262	1262	1262	2524	2524
SR11	PA-ID2	AC-20	N/A	A2	4.5	150 x 150	Unc. Comp.	0	1362	1362	1362	1362	2724	2724
SR11	PA-ID3	AC-20	N/A	A3MF+	4.0	150 x 150	Unc. Comp.	0	1174	1174	1174	1174	2348	2348
SR11	PA-ID3	AC-20	N/A	A3MF+	3.8	150 x 150	Unc. Comp.	0	1216	1216	1216	1216	2432	2432
SR11	PA-ID3	AC-20	N/A	A3MF+	4.2	150 x 150	Unc. Comp.	0	1165	1165	1165	1165	2330	2330
SR11	PA-ID3	AC-20	N/A	A3MF+	3.9	150 x 150	Unc. Comp.	0	1171	1171	1171	1171	2342	2342
SR11	PA-ID3	AC-20	N/A	A3	3.9	150 x 150	Unc. Comp.	0	1192	1192	1192	1192	2384	2384
SR11	PA-ID3	AC-20	N/A	A3	4.2	150 x 150	Unc. Comp.	0	1214	1214	1214	1214	2428	2428

Project	Agg. Grad.	Binder	N-design	Mix Code	Air Voids	Spec. Size, Dia. by Ht.	Test Type	Con. Stress	p	q	p, Corr. For Voids	q, Corr. For Voids	Dev. Stress	Dev. Str., Corr. For Voids
					%	mm		kPa	kPa	kPa	kPa	kPa	kPa	kPa
SR11	PA-ID3	AC-20	N/A	A3	4.4	150 x 150	Unc. Comp.	0	1229	1229	1229	1229	2458	2458
SR11	PA-ID3	AC-20	N/A	A3	4.1	150 x 150	Unc. Comp.	0	1204	1204	1204	1204	2408	2408
SR11	PA-ID3	AC-20	N/A	A3	4.1	150 x 150	Unc. Comp.	0	1268	1268	1268	1268	2536	2536
NY	12.5-mm	PG 58-28	76	NY76	4.2	150 x 150	Unc. Comp.	0	865	865	865	865	1730	1730
NY	12.5-mm	PG 58-29	76	NY76	4.4	150 x 150	Unc. Comp.	0	850	850	850	850	1700	1700
NY	12.5-mm	PG 58-30	76	NY76	4.2	150 x 150	Unc. Comp.	0	872	872	872	872	1744	1744
NY	12.5-mm	PG 58-31	96	NY96	4.1	150 x 150	Unc. Comp.	0	1012	1012	1012	1012	2024	2024
NY	12.5-mm	PG 58-32	96	NY96	4.2	150 x 150	Unc. Comp.	0	1023	1023	1023	1023	2046	2046
NY	12.5-mm	PG 64-28	109	NY109	4.2	150 x 150	Unc. Comp.	0	1163	1163	1163	1163	2326	2326
NY	12.5-mm	PG 64-29	109	NY109	4.1	150 x 150	Unc. Comp.	0	1127	1127	1127	1127	2254	2254
NY	12.5-mm	PG 64-30	126	NY126	4.4	150 x 150	Unc. Comp.	0	1205	1205	1205	1205	2410	2410
NY	12.5-mm	PG 64-31	126	NY126	4.2	150 x 150	Unc. Comp.	0	1213	1213	1213	1213	2426	2426
SR11	12.5-mm	PG 76-28	N/A	S2	3.7	100 x 150	IDT Str.	0	442	884	442	884	1768	1768
SR11	12.5-mm	PG 76-29	N/A	S2	4.2	100 x 150	IDT Str.	0	507	1015	507	1015	2030	2030
SR11	12.5-mm	PG 76-30	N/A	S2	3.9	100 x 150	IDT Str.	0	463	925	463	925	1850	1850
SR11	12.5-mm	PG 76-31	N/A	S2	3.8	100 x 150	IDT Str.	0	434	869	434	869	1738	1738
SR11	12.5-mm	PG 76-32	N/A	S2	3.8	100 x 150	IDT Str.	0	452	905	452	905	1810	1810
SR11	12.5-mm	PG 76-33	N/A	S3	4.0	100 x 150	IDT Str.	0	515	1030	515	1030	2060	2060
SR11	12.5-mm	PG 76-34	N/A	S3	4.0	100 x 150	IDT Str.	0	503	1006	503	1006	2012	2012
SR11	12.5-mm	PG 76-35	N/A	S3	3.9	100 x 150	IDT Str.	0	481	963	481	963	1926	1926
SR11	12.5-mm	PG 76-36	N/A	S3	3.9	100 x 150	IDT Str.	0	443	886	443	886	1772	1772
SR11	PA-ID2	AC-20	N/A	A2	3.8	100 x 150	IDT Str.	0	378	755	378	755	1510	1510
SR11	PA-ID2	AC-20	N/A	A2	4.2	100 x 150	IDT Str.	0	376	752	376	752	1504	1504
SR11	PA-ID2	AC-20	N/A	A2	4.2	100 x 150	IDT Str.	0	385	770	385	770	1540	1540
SR11	PA-ID2	AC-20	N/A	A2	4.0	100 x 150	IDT Str.	0	398	796	398	796	1592	1592
SR11	PA-ID3	AC-20	N/A	A3MF+	3.7	100 x 150	IDT Str.	0	397	793	397	793	1586	1586
SR11	PA-ID3	AC-20	N/A	A3MF+	3.6	100 x 150	IDT Str.	0	397	794	397	794	1588	1588
SR11	PA-ID3	AC-20	N/A	A3MF+	3.8	100 x 150	IDT Str.	0	399	798	399	798	1596	1596
SR11	PA-ID3	AC-20	N/A	A3MF+	4.0	100 x 150	IDT Str.	0	368	737	368	737	1474	1474
SR11	PA-ID3	AC-20	N/A	A3	4.3	100 x 150	IDT Str.	0	390	781	390	781	1562	1562
SR11	PA-ID3	AC-20	N/A	A3	4.5	100 x 150	IDT Str.	0	380	761	380	761	1522	1522
SR11	PA-ID3	AC-20	N/A	A3	4.1	100 x 150	IDT Str.	0	418	835	418	835	1670	1670

Project	Agg. Grad.	Binder	N-design	Mix Code	Air Voids	Spec. Size, Dia. by Ht.	Test Type	Con. Stress	p	q	p, Corr. For Voids	q, Corr. For Voids	Dev. Stress	Dev. Str., Corr. For Voids
					%	mm		kPa	kPa	kPa	kPa	kPa	kPa	kPa
SR11	PA-ID3	AC-20	N/A	A3	4.2	100 x 150	IDT Str.	0	407	813	407	813	1626	1626
NY	12.5-mm	PG 58-28	76	NY76	4.1	100 x 150	IDT Str.	0	199	397	199	397	794	794
NY	12.5-mm	PG 58-28	76	NY76	3.8	100 x 150	IDT Str.	0	181	361	181	361	722	722
NY	12.5-mm	PG 58-28	76	NY76	4.2	100 x 150	IDT Str.	0	215	429	215	429	858	858
NY	12.5-mm	PG 58-28	76	NY76	4.1	100 x 150	IDT Str.	0	196	393	196	393	786	786
NY	12.5-mm	PG 58-28	96	NY96	4.2	100 x 150	IDT Str.	0	252	503	252	503	1006	1006
NY	12.5-mm	PG 58-28	96	NY96	4.3	100 x 150	IDT Str.	0	271	543	271	543	1086	1086
NY	12.5-mm	PG 64-28	109	NY109	4.1	100 x 150	IDT Str.	0	244	487	244	487	974	974
NY	12.5-mm	PG 64-28	109	NY109	3.9	100 x 150	IDT Str.	0	262	524	262	524	1048	1048
NY	12.5-mm	PG 64-28	126	NY126	3.7	100 x 150	IDT Str.	0	309	618	309	618	1236	1236
NY	12.5-mm	PG 64-28	126	NY126	3.5	100 x 150	IDT Str.	0	275	550	275	550	1100	1100